THE NAUTILUS

Volume 133, Numbers 3–4
November 27, 2019
ISSN 0028-1344

A quarterly devoted to malacology.

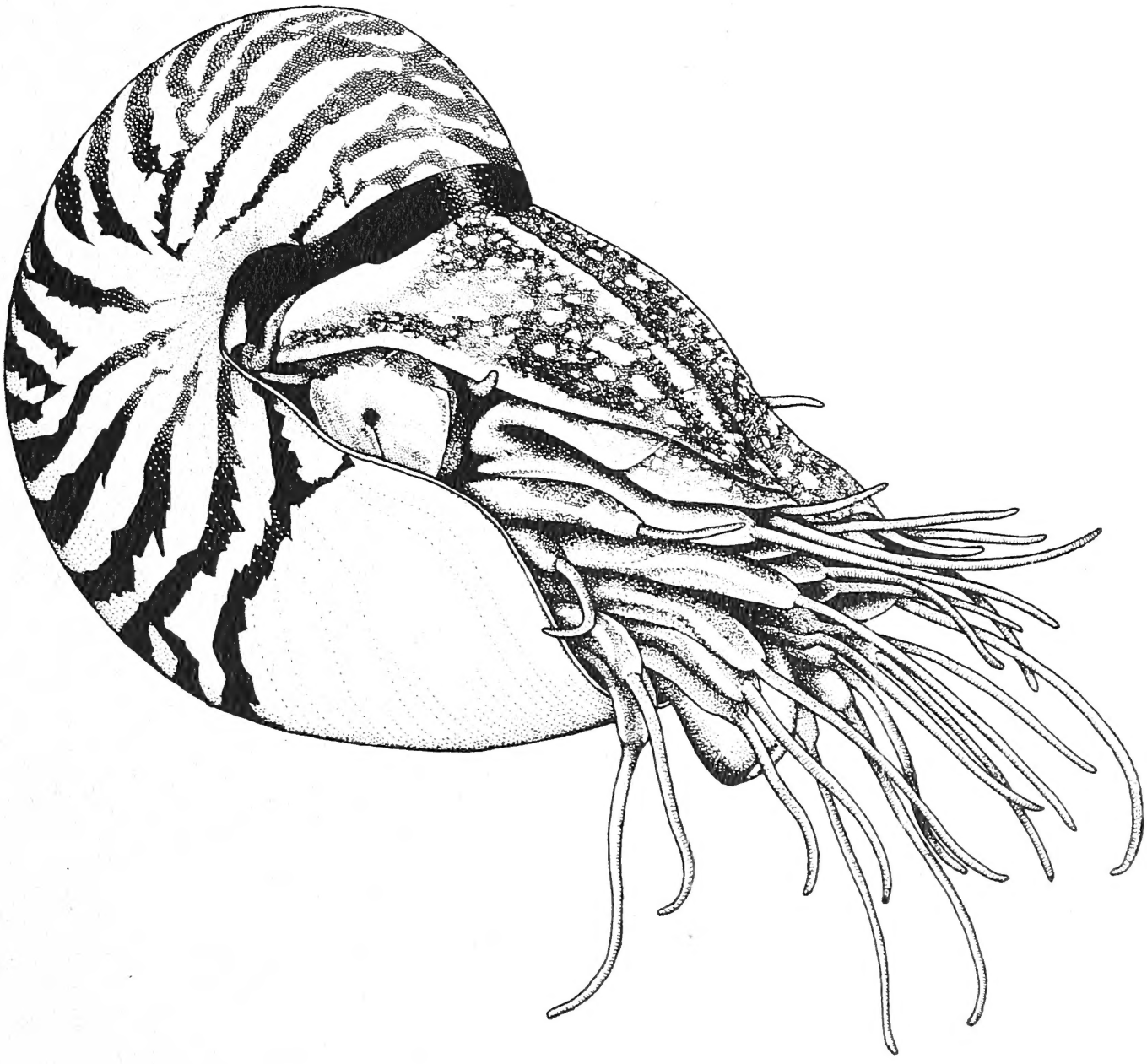

SUBSCRIPTION INFORMATION

The subscription rate for volume 134 (2020) is US $65.00 for individuals, US $102.00 for institutions. Postage outside the United States is an additional US $10.00 for regular mail and US $28.00 for air delivery. All orders should be accompanied by payment and sent to: THE NAUTILUS, P.O. Box 1580, Sanibel, FL 33957, USA, (239) 395-2233.

Change of address: Please inform the publisher of your new address at least 6 weeks in advance. All communications should include both old and new addresses (with zip codes) and state the effective date.

THE NAUTILUS (ISSN 0028-1344) is published quarterly by The Bailey-Matthews National Shell Museum, 3075 Sanibel-Captiva Road, Sanibel, FL 33957.

Periodicals postage paid at Sanibel, FL, and additional mailing offices.

POSTMASTER: Send address changes to: THE NAUTILUS
P.O. Box 1580
Sanibel, FL 33957

THE NAUTILUS

Volume 133, Numbers 3–4
November 27, 2019
ISSN 0028-1344

CONTENTS

STATEMENT OF OWNERSHIP, MANAGEMENT, AND CIRCULATION

1. Publication Title, THE NAUTILUS.
2. Publication No. 0028-1344.
3. Filing Date, November 11, 2019.
4. Issue Frequency, Quarterly.
5. No. of Issues Published Annually, Four.
6. Annual Subscription Price, US $102.00.
7. Complete Mailing Address of Known Office of Publication, 3075 Sanibel-Captiva Road, Sanibel, FL 33957 USA
8. Complete Mailing Address of Headquarters, same as 7.
9. Full Names and Complete Mailing Addresses of Publisher, The Bailey-Matthews Shell Museum, 3075 Sanibel-Captiva Road, Sanibel, FL 33957 USA
   Editor, Dr. José H. Leal, address as above.
10. Owner, Shell Museum and Educational Foundation, Inc., address as above.
11. Known Bondholders, Mortgagees, and Other Security Holders Owning or Holding 1 Percent or More of Total Amount of Bonds, Mortgages, or Other Securities, None.
12. The purpose, function, and nonprofit status of this organization and the tax exempt status for federal income tax purposes has not changed during the preceding 12 months.
13. Publication Name, THE NAUTILUS.
14. Issue Date for Circulation Data Below, August 8, 2019

15. Extent and Nature of Circulation	Average 12 months	Single Issue
a. Total Number of Copies	260	260
b. Paid Circulation		
1. Paid/Requested Outside-County Mail Subscriptions	215	214
2. Paid In-County Subscriptions	0	0
3. Sales Through Dealers and Carriers, Street Vendors, Counter Sales, and Other Non-USPS Paid Distribution	0	0
4. Other Classes Mailed Through the USPS	14	15
c. Total Paid and/or Requested Circulation	229	229
d. Free Distribution by Mail		
1. Outside-County	11	11
2. In-County	0	0
3. Other Classes Mailed Through the USPS	0	0
4. Free distribution outside the Mail	0	0
e. Total Free or Nominal Rate Distribution	11	11
f. Total Distribution	240	240
g. Copies not Distributed	20	12
h. Total	260	252
i. Percent Paid Total	95%	91%

16. Electronic Copy Circulation		
a. Paid Electronic Copies	0	0
b. Total Paid Print Copies + Paid Electronic Copies	229	229
c. Total Print Distribution + Paid Electronic Copies	240	240
d. Percent Paid (Both Print & Electronic Copies)	95%	95%

The complete mitochondrial genome of *Neptuneopsis gilchristi* G.B. Sowerby III, 1898 (Neogastropoda: Volutidae: Calliotectinae)

M. G. Harasewych[1]
Makiri Sei
Herman H. Wirshing
Department of Invertebrate Zoology, MRC-163
National Museum of Natural History
Smithsonian Institution
P.O. Box 37012
Washington, DC 20013-7012 USA

Vanessa L. González
Global Genome Initiative
National Museum of Natural History
Smithsonian Institution
P.O. Box 37012
Washington, DC 20013-7012 USA

Juan E. Uribe
Department of Invertebrate Zoology, MRC-163
National Museum of Natural History
Smithsonian Institution
P.O. Box 37012
Washington, DC 20013-7012, USA

ABSTRACT

We report the complete mitochondrial genome of *Neptuneopsis gilchristi* G.B. Sowerby III, 1898, the type species of the monotypic genus *Neptuneopsis*. This mitogenome is 15,312 bp in length and has a GC content of 31.3%. The gene order of the 13 protein-coding genes, 2 ribosomal RNA genes, and 22 transfer RNA genes, is identical to that of most neogastropods other than of several conoidean taxa, which differ only in the location of one or more tRNA genes. The potential origin of replication is located in a 127 bp non-coding region between tRNA-Phe and COX3 that has a high A + T content (77.9%). Phylogenetic analyses using maximum likelihood and Bayesian inference with nucleotide sequences of all protein-coding and ribosomal genes show *Neptuneopsis* to be sister to the few volutid species for which complete or partial mitogenome data are available. *Neptuneopsis gilchristi* has an operculum and a triserial radula, while the other volutids in our analyses have lost the operculum and have a derived uniserial radula.

Keywords: Gastropoda, mitogenome, phylogeny, gene order

INTRODUCTION

The neogastropod family Volutidae comprises a group of predatory marine gastropods that inhabit sand and mud substrates from the intertidal zone to abyssal plains, from the tropics to polar seas. Like many neogastropod families, Volutidae has origins in the early Late Cretaceous (Cenomanian) (Stephenson, 1952; Pojarkova, 1984; Tracey et al., 1993; Fossilworks, 2019). The World Register of Marine Species (WoRMS, 2019) lists 1,640 living and fossil species-level taxa and 115 living and fossil genus-level taxa attributed to this family. Pilsbry and Olsson (1954) reviewed the early taxonomic history of Volutidae and partitioned the family into 12 subfamilies and 8 tribes, acknowledging this to be a tentative effort. The most recent classification (Bouchet et al., 2017:349) recognizes 10 subfamilies (2 extinct) and 11 tribes.

Earlier classifications based on morphological and anatomical data (e.g., Thiele, 1929; Wenz, 1943) included Volutidae in the superfamily Volutoidea, together with the families Olividae, Mitridae, Turbinellidae, Harpidae, Marginellidae, and Cancellariidae, while subsequent classifications have variously distributed these families among the rachiglossan neogastropods (see Harasewych et al., 1997: fig. 2). The most recent classification (Bouchet et al., 2017: 349, 379) based on molecular data (Fedosov et al., 2015) includes only Volutidae and Cancellariidae in Volutoidea, with the remaining families either elevated to superfamilies or unassigned to superfamily.

The family Volutidae has been sparsely represented in morphological and molecular investigations of neogastropod phylogeny. In this study, we report the complete mitochondrial genome of *Neptuneopsis gilchristi* G.B. Sowerby III, 1898, a member of the subfamily Calliotectinae. It represents the second complete mitogenome of a volutid to be determined. Features such as genome length and gene order are compared to those of other neogastropods, and the phylogenetic position of *Neptuneopsis* within Volutidae is inferred under both maximum likelihood (ML) and Bayesian frameworks based on mitochondrial protein-coding and RNA genes.

MATERIALS AND METHODS

DNA Extraction and Sanger Sequencing: Genomic DNA (gDNA) was extracted from a 40 mg section of proboscis wall obtained from an alcohol-preserved specimen of *Neptuneopsis gilchristi* [Natal Museum, V1106; South Africa, South of Cape St. Blaize (34°47' S, 22°10' E), dredged in 97 m, Stn. A17383, NMDP, R/V AFRICANA, 6 May 1995] using the AutoGenprep 965 (Autogen, Holliston, MA, USA). Manufacturer-provided proteinase K (Autogen) was used for initial tissue lysis,

[1] Corresponding author: Harasewych@si.edu

which was run overnight at 56°C with continuous agitation. Portions of cytochrome *c* oxidase I (COXI) and 16S rRNA genes were PCR-amplified and Sanger-sequenced using the primers and protocols in Harasewych (2018). These two mitochondrial gene fragments were used as scaffolds for the assembly of the *N. gilchristi* mitogenome (see **Assembly** below).

Library Construction and Illumina Sequencing: Extracted gDNA was visualized on a 1.5% agarose gel, and quantified using a Qubit dsDNA HS Assay Kit (ThermoFisher, Pittsburg, PA). After quantification, gDNA was sonicated using the Covaris ME220 with microtube-50 AFA fiber screw-caps (Covaris, Woburn, MA) targeted for 350bp fragments. Sonicated gDNA was then cleaned using Kapa Pure Beads (KAPA Biosystems, Wilmington, MA) at a 0.9X beads-to-sample ratio, which targeted fragments >250bp. Size-selected gDNA was then quantified with Qubit dsDNA HS Assay Kit, and the Agilent 2200 TapeStation (Agilent, Santa Clara, CA) was used to validate gDNA size selection.

Total gDNA libraries were prepared using the NEBNext Ultra II DNA Library Prep Kit for Illumina together with the NEBNext Multiplex Oligos for Illumina (New England BioLabs, Ipswich, MA). Size selection of adaptor-ligated libraries (400–500 bp) and adaptor/PCR cleanups were performed using Kapa Pure Beads, and library size was validated with the Agilent 2200 Tape Station. Libraries were quantified using qPCR (ViiA 7, ThermoFisher) to ensure generation of adaptor-ligated libraries. A 4nM library concentration was denatured for clonal amplification and sequenced on an Illumina MiSeq (Illumina, San Diego, CA) with MiSeq Reagent Kit v3 at the Smithsonian National Museum of Natural History's Laboratories of Analytical Biology.

Assembly: Low quality reads were removed using TrimGalore v. 0.6.3 dev (https://github.com/FelixKrueger/TrimGalore), with thresholds for minimum Phred scores set to 20 and minimum read lengths set to 20 bp. The *N. gilchristi* mitogenome was assembled using Geneious Prime® 2019.2.1 (http://www.geneious.com) using the following protocol: Sanger-sequenced COXI and 16S rRNA gene fragments were used as scaffolds using the "map to reference" tool with "minimum overlap identity" set to 98–99% and "minimum overlap" set to

Table 1. List of taxa used in phylogenetic analyses, their GenBank accession numbers, source of sequence data, and size of the entire mitogenome. Taxon names as well as their superfamily and family assignments have been updated according to WoRMS (2019). * Indicates that only a partial mitogenome sequence was available.

Superfamily	Family	Taxon	GenBank No.	Source	length (bp)
OUTGROUPS - LITTORINIMORPHA					
Stromboidea	Strombidae	*Lobatus gigas*	NC_024932	Marques et al 2014	15,461
Naticoidea	Naticidae	*Naticarius hebraeus*	NC_028002	Osca et al. 2015	15,384
Tonnoidea	Cymatiidae	*Monoplex parthenopeus*	NC_013247	Cunha et al. 2009	15,270
Tonnoidea	Charoniidae	*Charonia lampas*	NC_037188	Cho et al. 2017	15,330
Tonnoidea	Cassidae	*Galeodea echinophora*	NC_028003	Osca et al. 2015	15,388
NEOGASTROPODA					
Volutoidea	Cancellariidae	*Bivetiella cancellata*	NC_013241	Cunha et al. 2009	16,648
Volutoidea	Volutidae	*Neptuneopsis gilchristi*	MN125492	This study	15,312
Volutoidea	Volutidae	*Cymbium olla*	NC_013245	Cunha et al. 2009	15,375
Volutoidea	Volutidae	*Alcithoe lutea*	JN182219	Hills et al. 2011	7,689 *
Volutoidea	Volutidae	*Alcithoe benthicola*	JN182217	Hills et al. 2011	7,692 *
Volutoidea	Volutidae	*Amoria hunteri*	JN182226	Hills et al. 2011	7,728 *
Volutoidea	Volutidae	*Cymbiola pulchra*	JN182216	Hills et al. 2011	7,733 *
Muricoidea	Muricidae	*Bolinus brandaris*	NC_013250	Cunha et al. 2009	15,380
Muricoidea	Muricidae	*Rapana venosa*	NC_011193	Sun & Yang 2014	15,271
Muricoidea	Muricidae	*Reishia clavigera*	NC_010090	Ki et al. 2010	15,285
Olivoidea	Ancellariidae	*Amalda northlandica*	NC_014403	McComish et al. 2010	15,354
Unassigned	Babyloniidae	*Babylonia areolata*	NC_023080	Chen & Ke, unpublished	15,445
Unassigned	Babyloniidae	*Babylonia lutosa*	NC_028628	Xiong et al. 2015	15,346
Buccinoidea	Columbellidae	*Columbella adansoni*	KP716637	Osca et al. 2015	16,272
Buccinoidea	Nassariidae	*Tritia reticulatus*	NC_013248	Cunha et al. 2009	15,271
Buccinoidea	Buccinidae	*Neptunea arthritica*	KU246047	Hao et al. 2016	15,256
Buccinoidea	Buccinidae	*Buccinum undatum*	NC_040940	Jonsson et .al. 2019	15,265
Conoidea	Conidae	*Californiconus californicus*	NC_032377	Uribe et al. 2016	15,444
Conoidea	Conidae	*Conus borgesi*	NC_013243	Cunha et al. 2009	15,536
Conoidea	Conidae	*Conus textile*	NC_008797	Bandyopadhyay et al. 2008	15,562
Conoidea	Terebridae	*Oxymeris dimidiata*	NC_013239	Cunha et al. 2009	16,513
Conoidea	Fussiturridae	*Fusiturris similis*	NC_013242	Cunha et al. 2009	15,595
Conoidea	Turridae	*Iotyrris cerithiformis*	NC_008098	Bandyopadhyay et al. 2006	15,380
Conoidea	Turridae	*Gemmuloborsonia moosai*	NC_038183	Uribe et al. 2018	15,541

30–40 bp. An initial iterate, using the "fine tuning" option tab, was set to 5X to confirm adequate initial assembly to scaffolds. The 16S rRNA fragment did not scaffold well, and, therefore, only COXI was used for subsequent assembly iterations. Three–five iterations of 3X and 40X were needed before an assembled contig of >15kb, the mitogenome size-approximation based on related taxa, was acquired. The size and sequence of the non-coding region, between the tRNA-Phe and COX3, was confirmed using standard PCR and Sanger sequencing, with primers derived from within the flanking genes: NEPTtrn-Phe F – 5' GGT GGT AAA CAT ATC TTA AGA TAC G – 3' and NEPTcox3 R – 5' AAC TAA GTG GAA TGG ATT ACG TCT C.

Genome Annotation: Mitochondrial elements were annotated using MITOS (Bernt et al., 2013), ARWEN (Laslett and Canbäck, 2008) and the ORF finder in Geneious.

Phylogenetic Analyses: All 13 protein-coding and both ribosomal genes from selected neogastropod and outgroup mitochondrial genomes (Table 1) were used to determine the phylogenetic relationships of *N. gilchristi*. Gene alignments were run in MAFFT v7 (Katoh et al., 2019) and ambiguous positions removed using GBlocks, v.0.91b (Castresana, 2000). The best-fit evolutionary models and partition scheme were selected using ModelFinder (Kalyaanamoorthy et al., 2017) through IQ-TREE v.1.6.1 (Nguyen et al., 2014) with the option

Table 2. Position (start, stop), strand direction (+/-) and lengths (bp) of the genes in the mitochondrial genome of *Neptuneopsis gilchristi* G.B. Sowerby III, 1898 [15,312 bp; GenBank MN125492], initiation and termination codons (Init/Term) for protein-coding genes, as well as their amino acid sequence lengths (Laa). Standard abbreviations for protein coding genes are used. Both three and one letter abbreviations are listed for tRNA's, along with the codon used. The numbers of intergenic nucleotides (Ign) are shown. Negative numbers indicate overlap of genes.

Gene	Start	Stop	Strand Directionn	Length (bp)	Init /Term	Laa	Ign
COX1	1	1,542	+	1,542	ATG/TAA	513	11
COX2	1,554	2,240	+	687	ATG/TAA	228	-3
tRNA-Asp (D) (gtc)+	2,238	2,308	+	71			0
ATP8	2,309	2,467	+	159	ATG/TAA	52	5
ATP6	2,473	3,168	+	696	ATG/TAG	231	31
tRNA-Met (M) (cat)*	3,266	3,200	–	67			-3
tRNA-Tyr (Y) (gta)+	3,330	3,264	–	67			31
tRNA-Cys (C) (gca)*	3,395	3,332	–	64			-2
tRNA-Trp (W) (tca)+	3,461	3,394	–	68			-2
tRNA-Gln (Q) (ttg)+	3,525	3,460	–	66			0
tRNA-Gly (G) (tcc)+	3,594	3,526	–	69			-2
tRNA-Glu (E) (ttc)+	3,659	3,593	–	67			0
12S rDNA	3,660	4,615	+	956			0
tRNA-Val (V) (tac)+	4,616	4,683	+	68			0
16S rDNA	4,684	6,035	+	1,352			0
tRNA-Leu (L1)(tag)+	6,036	6,106	+	71			0
tRNA-Leu (L2)(taa)*	6,107	6,175	+	69			0
NAD1	6,176	7,117	+	942	ATG/TAA	313	0
tRNA-Pro (P) (tgg)*	7,118	7,189	+	72			0
NAD6	7,190	7,690	+	501	ATG/TAA	166	5
CYT B	7,696	8,835	+	1140	ATG/TAA	379	6
tRNA-Ser(S2)(tga)+	8,842	8,909	+	68			10
tRNA-Thr (T) (tgt)*	8,984	8,920	–	65			9
NAD4L	8,994	9,290	+	297	ATG/TAG	98	17
NAD4	9,308	10,657	+	1350	ATT/TAG	449	2
tRNA-His (H)(gtg)+	10,660	10,726	+	67			26
NAD5	10,753	12,447	+	1,695	ATT/TAA	564	10
tRNA-Phe (F)(gaa)+	12,458	12,5244	+	67			127
COX3	12,652	13,431	+	780	ATG/TAA	259	28
tRNA-Lys (K) (ttt)+	13,460	13,528	+	69			4
tRNA-Ala (A) (tgc)*	13,533	13,600	+	68			11
tRNA-Arg (R)(tcg)*	13,612	13,680	+	69			6
tRNA-Asn (N)(gtt)*	13,687	13,754	+	68			8
tRNA-Ile (I) (gat)+	13,763	13,830	+	68			3
NAD3	13,834	14,187	+	354	ATG/TAG	118	0
tRNA-Ser (S1)(gct)*	14,188	14,255	+	68			0
NAD2	14,256	29	+	1086	ATG/TAA	361	-29

For tRNA's * indicates that ARWEN the same as MITOS.
For tRNA's + indicates that ARWEN selected over MITOS.

"-m TESTONLYMERGE" and Bayesian Information Criterion (BIC).

Phylogenetic analyses, using a data matrix concatenated in Geneious that included 12,636 nucleotide positions, were performed with MrBayes v3.1.2 (Ronquist and Huelsenbeck, 2003) running four MCMC chains for two million generations, sampling every 1,000 and discarding the first 25% as burn-in. Convergence of the trees was determined using TRACER v1.6 (Rumbaut et al., 2007); and IQ-TREE v1.6.1 using a combination of rapid hill-climbing and stochastic perturbation methods with a total of 1,000 pseudoreplicates of bootstrap to assess robustness of the inferred tree.

RESULTS

Genome Content and Organization: The Illumina sequencing run produced a total of 51,544,678 reads for this species. After filtering and removing low-quality data, 50,964,146 reads (Phred scores ≥ 20, length ≥ 20 bp) remained with an average length of 193.2 bp (SD 77.8). Of these 12,954 mapped to the mitochondrial genome. Coverage ranged from 115X to 345X per site (mean = 213.5; SD = 38.1).

The mitochondrial genome of *Netuneopsis gilchristi* reconstructed from these data is a double-stranded circular molecule 15,312 bp in length (GenBank Acc. No. MN125492), composed of 31.0% A, 37.7% T, 15.8% C, and 15.6% G. It contains 13 protein-coding genes, two ribosomal RNA genes and 22 tRNA genes (Table 2, Fig. 1). Of these, 29 genes are coded on the heavy strand (+ strand) and only 8 tRNA genes, including the cluster MYCWQGE (tRNA-M, tRNA-Y, tRNA-C, tRNA-W, tRNA-Q, tRNA-G, and tRNA-E) and tRNA-T are coded on the light strand (– strand). The gene order in *N. gilchristi* corresponds to the consensus gene order shared by most caenogastropod (Osca et al., 2015: 122) and neogastropod (Cunha et al., 2009: 210, Fig. 1) mitogenomes. Known exceptions to this gene order are limited to unrelated tRNA translocations and inversions within Conoidea (Cunha et al., 2009; Uribe et al., 2016: fig. 1; Uribe et al., 2018: fig. 2).

Gene overlaps total 41 bp at 6 gene junctures, the longest (29 bp) between NAD2 and COX1. There are 19 intergenic regions (350 bp in total, 2.3 % of the mitogenome) ranging from 2 to 127 bp, the largest between tRNA-Phe and COX3 (Table 2).

The potential origin of replication (POR) is located in a 127 bp non-coding region between tRNA-Phe and COX3, which has a high A + T content (77.9%).

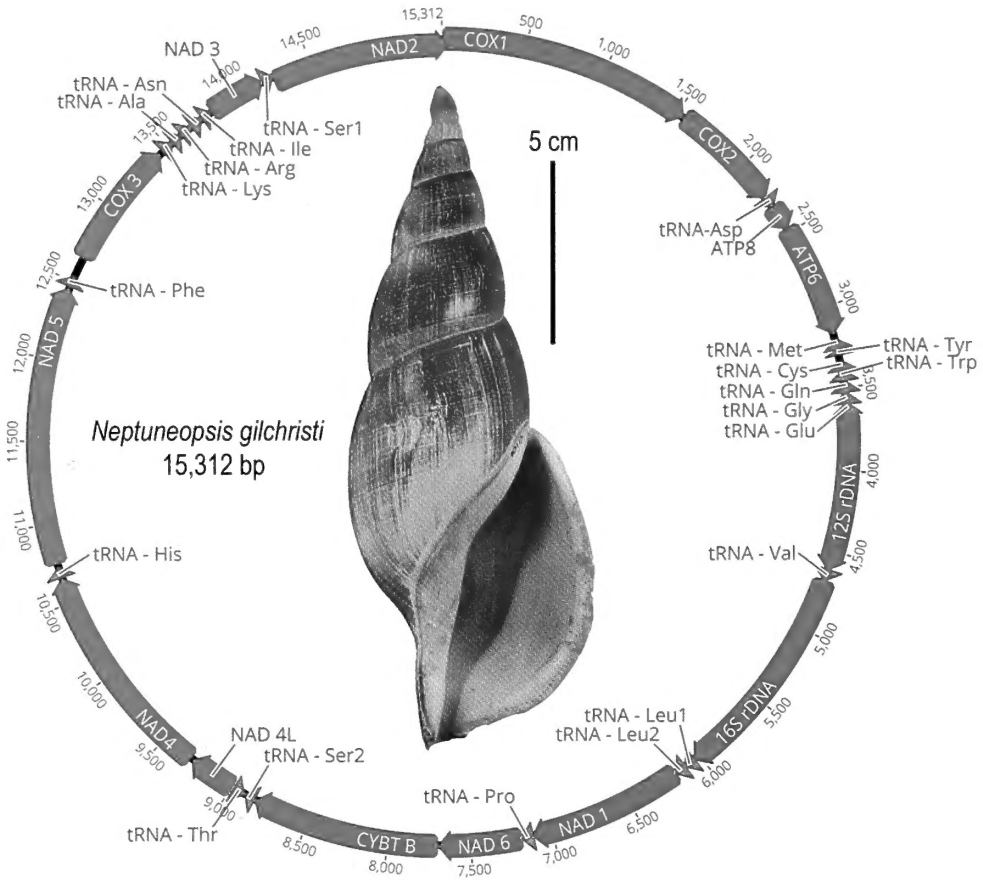

Figure 1. Map of the mitochondrial genome of *Neptuneopsis gilchristi* (GenBank Acc. no. MN125492). Arrows indicate the direction of transcription. Protein-coding genes are in green, ribosomal genes in red and transfer RNA genes in purple.

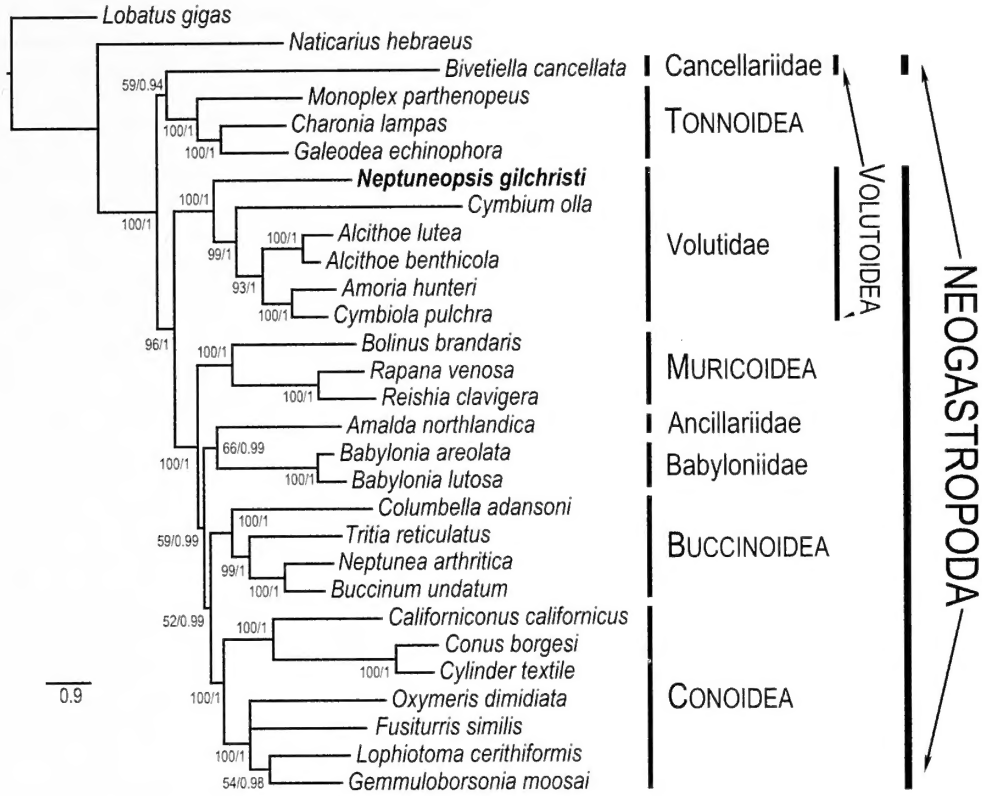

Figure 2. Phylogenetic relationships of *Neptuneopsis gilchristi* based on maximum likelihood and Bayesian analyses of nucleotide sequences of mitochondrial protein-coding and ribosomal genes. Branch support shown as maximum likelihood bootstrap values (when ≥ 50) / Bayesian posterior probability (when ≥ 0.7).

Protein coding genes comprise 73.3% of the entire genome (11,229 bp). The most common start codon is ATG, occurring in all genes except ND4 and ND5, which use the ATT start codon. The stop codon TAA is used in nine genes and the TAG stop codon in four genes. Both the large ribosomal gene (16S rRNA, 1352 bp) and the small ribosomal gene (12S rRNA, 956 bp) (total = 2,308 bp, 15.1% of mitogenome) occur on the heavy strand. Of the 22 t-RNAs, 14 are on the heavy strand, 8 on the light strand. The total length of the tRNAs is 1496 bp, 9.8% of mitogenome.

Phylogenetic Analyses: Phylogenetic analyses of the concatenated nucleotide sequences for all protein-coding and ribosomal RNA genes using both maximum likelihood and Bayesian inference each produced a single tree that was fully resolved, and in which most nodes were well supported. The two trees were congruent except for the relative positions of *Oxymeris* and *Fusiturris*, among the non-conid Conoidea (Figure 2).

DISCUSSION

The mitogenome of *Neptuneopsis gilchristi* (15,312 bp) is 63 bp shorter than that of *Cymbium olla*, the only other volutid for which a complete mitogenome is known. The order and strand orientation of the mitochondrial genes is the same for both species, and also matches the portion (>7,600 bp) of the mitogenome between ND3 and tRNA-Leu2 that has been reported for 11 species of *Alcithoe*, *Amoria hunteri*, and *Cymbiola pulchra* (Hills et al., 2011: Table 1, Fig. 1). The ND2 gene overlaps the COX1 gene by 29 bp for all volutid species reported to date except *Cymbium olla*, which has a 17 bp gap between the two genes.

Analyses using both maximum likelihood and Bayesian inference (Figure 2) strongly support the monophyly of the superfamilies Conoidea, Buccinoidea, Muricoidea, and Tonoidea. The family Volutidae is also recovered as monophyletic with strong support, but not the superfamily Volutoidea, as the sole cancellariid in the dataset appears more closely related to Tonnoidea, although without significant support. A similar result was obtained by Cunha et al. (2009: fig. 3) and Osca et al. (2015: fig. 2) when analyzing nucleotide sequences of complete mitochondrial genomes. The monophyly of Neogastropoda has often been contradicted in multiple molecular studies (for review, see Ponder et al., 2008: 368), as Tonnoidea typically are included among Neogastropoda (Osca et al., 2015; Strong et al., 2019).

Neptuneopsis emerges as the earliest branching of the few volutid taxa for which data on a significant portion of the mitogenome are available. This is concordant with relationships based on morphology, as *Neptuneopsis* is the

only taxon within this study that retains an operculum and a triserial radular ribbon, both considered plesiomorphic features within Volutidae (Pilsbry and Olsson, 1954). Of the remaining volutids, *Amoria hunteri* and *Cymbiola pulchra*, members of separate tribes within the subfamily Amoriinae, emerge as sister taxa, as do the congeners *Alcithoe lutea* and *A. benthicola*.

However, the two species of *Alcithoe* do not form a clade with *Cymbium olla*, although all three are classified in the subfamily Cymbiinae. It is unclear if this discrepancy may be due to the comparison of complete versus partial mitogenomes. Cunha and colleagues (2009: 210) noted the uneven contributions of various genes to phylogenetic resolution, with COX2, ATP6, and NAD4 being rated the highest, and COXI and ATP8 the lowest. We regard this mitogenome as being an incremental contribution toward a better understanding of the evolutionary history of Volutidae.

ACKNOWLEDGMENTS

We thank Dai Herbert, Linda Davis, and Igor Muratov of the KwaZulu-Natal Museum for making available the specimen used in this study, as well as for providing additional information and images. All laboratory work, sequencing and analyses were conducted in and with the support of the Laboratories of Analytical Biology (LAB) facilities of the National Museum of Natural History.

LITERATURE CITED

Bandyopadhyay, P.K., B.J. Stevenson, M.T. Cady, B.M. Olivera, and D.R. Wolstenholme. 2006. Complete mitochondrial DNA sequence of a conoidean gastropod, *Lophiotoma (Xenuroturris) cerithiformis*: gene order and gastropod phylogeny. Toxicon 48: 29–43.

Bandyopadhyay, P.K., B. J. Stevenson, J.-P. Ownby, M.T. Cady, M. Watkins, and B.M. Olivera. 2008. The mitochondrial genome of *Conus textile*, coxI–coxII intergenic sequences and conoidean evolution. Molecular Phylogenetics and Evolution 46: 215–223.

Bernt, M., A. Donath, F. Juhling, F. Externbrink, C. Florentz, G. Fritsch, J. Pütz, J., M. Middendorf, and P.F. Stadler. 2013. MITOS: improved *de novo* metazoan mitochondrial genome annotation. Moleular Phylogenetics and Evolution 69: 313–319.

Bouchet, P., J-P. Rocroi, B. Hausdorf, A. Kaim, Y. Kano, A. Nutzel, P. Parkhaev, M. Schrodl, and E. E. Strong. 2017. Revised classification, nomenclator and typification of gastropod and monoplacophoran families. Malacologia 61(1–2): 1–526.

Castresana, J. 2000. Selection of conserved blocks from multiple alignments for their use in phylogenetic analysis. Molecular Biology and Evolution 17: 540–552.

Cho, I.Y., K.Y. Kim, C.H. Yi, I.H. Kim, Y.H. Jung, S.J. Hwang, J. Bae, M. Yoon, and M.S. Kim. 2017. Full-length mitochondrial genome of the triton trumpet *Charonia lampas* (Littorinimorpha: Ranellidae). Mitochondrial DNA Part B 2: 759–760.

Cunha, R.L., C. Grande, and R. Zardoya. 2009. Neogastropod phylogenetic relationships based on entire mitochondrial genomes. BMC Evolutionary Biology 9: 210.

Fedosov, A., N. Puillandre, Y. Kantor, and P. Bouchet. 2015. Phylogeny and systematics of mitriform gastropods (Mollusca: Gastropoda: Neogastropoda). Zoological Journal of the Linnean Society 175: 336–359.

Fossilworks. 2019. Available from http://fossilworks.org. Accessed 2019-06-03.

Hao, Z., L. Yang, Y. Zhan, Y. Tian, J. Mao, L. Wang, and Y. Chang. 2016. The complete mitochondrial genome of *Neptunea arthritica cumingii* Crosse (Gastropoda: Buccinidae). Mitochondrial DNA Part B 1: 220–221.

Harasewych, M.G., S.L. Adamkewicz, J.A. Blake, D. Saudek, T. Spriggs, and C.J. Bult 1997. Neogastropod phylogeny: a molecular perspective. Journal of Molluscan Studies 63: 327–351.

Harasewych, M.G. 2019. *Tropidofusus ypotethys*: a new genus and species of Columbariidae (Mollusca: Gastropoda: Turbinelloidea). Molluscan Research 39: 148–158.

Hills, S.F.K., S.A. Trewick, and M. Morgan-Richards. 2011. Phylogenetic information of genes, illustrated with mitochondrial data from a genus of gastropod molluscs. Biological Journal of the Linnean Society 104: 770–785.

Jonsson, Z.O., S. Palsson, K.M. Westfall, H. Magnusdottir, J. Goodall, and E.B. Ornolfsdottir. 2019. The mitochondrial genome of common whelk *Buccinum undatum* (Neogastropoda: Buccinidae). Mitochondrial DNA Part B 4 (1): 458–460.

Kalyaanamoorthy, S., B.Q. Minh, T.K.F. Wong, A. von Haeseler, and L.S. Jermiin. 2017. ModelFinder: fast model selection for accurate phylogenetic estimates. Nature Methods 14: 587.

Katoh, K., J. Rozewicki, and K.D. Yamada. 2019. MAFFT online service: multiple sequence alignment, interactive sequence choice and visualization. Briefings in Bioinformatics 20(4): 1160-1166.

Kearse, M., R. Moir, A. Wilson, S. Stone-Havas, M. Cheung, S. Sturrock, S., Buxton, A. Cooper, S. Markowitz, C. Duran, T. Thierer, B. Ashton, P. Mentjies, and A. Drummond. 2012. Geneious Basic: an integrated and extendable desktop software platform for the organization and analysis of sequence data. Bioinformatics 28(12): 1647–1649.

Ki, J-S., Y-M. Lee, S-O. Jung, T. Horiguchi, H-S. Cho, and J-S. Lee. 2010. Mitochondrial genome of *Thais clavigera* (Mollusca: Gastropoda): affirmation of the conserved, ancestral gene pattern within mollusks. Molecular Phylogenetics and Evolution 54: 1016–1020.

Laslett, D. and B. Canbäck. 2008. ARWEN: a program to detect tRNA genes in metazoan mitochondrial nucleotide sequences. Bioinformatics 24: 172–175.

Marques, E. J., E.R. Castro, and J.F. Alzate. 2016. Mitochondrial genome of the endangered marine gastropod *Strombus gigas* Linnaeus, 1758 (Mollusca: Gastropoda). Mitochondrial DNA 27(2): 1516–1517.

McComish, B.J., S.F. Hills, P.J. Biggs, and D. Penny. 2010. Index-free *de novo* assembly and deconvolution of mixed mitochondrial genomes. Genome Biology and Evolution 2: 410–424.

Nguyen, L.T., H.A. Schmidt, A.von Haeseler, and B.Q. Minh. 2014. IQ-TREE: a fast and effective stochastic algorithm for estimating maximum-likelihood phylogenies. Molecular Biology and Evolution 32: 268–274.

Osca, D., J. Templado, and R. Zardoya. 2015. Caenogastropod mitogenomics. Molecular Phylogenetics and Evolution 93: 118–128.

Pilsbry, H.A. and A.A. Olsson. 1954. Systems of the Volutidae. Bulletins of American Paleontology 35: 275–306, pls. 25–28.

Pojarkova, Z.N. 1984. The Cenomanian and Turonian in Northeastern Central Asia. Cretaceous Research 5: 1–14.

Ponder, W.F., D.J. Colgan, J.M. Healy, A. Nützel, L.R.L. Simone, and E. E. Strong. 2008. Caenogastropoda. In: Ponder, W.F. and D.L. Lindberg (eds.), Molluscan Phylogeny and Evolution. University of California Press, Berkeley, pp. 331–383.

Ronquist, F. and J.P. Huelsenbeck. 2003. MrBayes 3: Bayesian phylogenetic inference under mixed models. Bioinformatics 19: 1572–1574.

Rambaut, A., A. Drummond, and M. Suchard. 2007. Tracer v1.6 (http://beast.bio.ed.ac.uk)

Sowerby, G.B., III. 1898. Description of a new South African marine gasteropod. Marine Investions in South Africa 5: 5–7.

Stephenson, L.W. 1952. Larger invertebrate fossils of the Woodbine Formation (Cenomanian) of Texas. U.S. Geological Survey Professional Paper 242: i-iv, 1-211, pls. 1–58.

Strong, E.E., N. Puillandre, A.G. Beu, M. Castelin, and P. Bouchet. 2019. Frogs, tuns and tritons – A molecular phylogeny and revised family classification of the predatory gastropod superfamily Tonnoidea. Molecular Phylogenetics and Evolution 130: 18–24.

Sun, X. and A. Yang. 2016. The complete mitochondrial genome of *Rapana venosa* (Gastropoda, Muricidae). Mitochondrial DNA Part A 27: 1471–1472.

Thiele, J. 1929. Handbuch der systematischen Weichtierkunde. Fischer, Jena. Tiel 1:1–376.

Tracey, S., J.A. Todd, and D.H. Erwin. 1993. Mollusca: Gastropoda. In: Benton, M.J. (ed.), The Fossil Record 2, Chapman and Hall, London: pp. 131–167.

Uribe, J.E., N. Puillandre, and R. Zardoya. 2016. Beyond *Conus*: Phylogenetic relationships of Conidae based on complete mitochondrial genomes. Molecular Phylogenetics and Evolution 107: 142–151.

Uribe, J.E., R. Zardoya, and N. Puillandre. 2018. Phylogenetic relationships of the conoidean snails (Gastropoda: Caenogastropoda) based on mitochondrial genomes. Molecular Phylogenetics and Evolution 127: 898–906.

Wenz, W. 1943. Gastropoda. In: O.H. Schindewolf (ed.) Handbuch der Paläozoologie. Band 6. Gebrüder Borntraeger, Berlin. Teil 6 :1201–1506.

WoRMS, 2019. World Register of Marine Species. Available from http://www.marinespecies.org at VLIZ. Accessed 2019-06-03.

Xiong, G., X. Ma, X.Q. Wang, D.L. Zhu, L.M. Wang, and Q. Qin. 2015. The complete mitochondrial genome of the *Babylonia lutosa*. Mitochondrial DNA 26: 187–188.

Post-glacial dispersal patterns of *Pyganodon grandis* (Bivalvia: Unionidae) into the lower Great Lakes watershed

Robert A. Krebs
Department of Biological, Geological, and Environmental Sciences
Cleveland State University
Cleveland, OH 44115-2406 USA
r.krebs@csuohio.edu

Lyuba E. Burlakova
Great Lakes Center
SUNY Buffalo State
Buffalo, NY 14222 USA

David T. Zanatta
Department of Biology
Institute for Great Lakes Research,
Central Michigan University
Mount Pleasant, MI 48859 USA

ABSTRACT

Pyganodon grandis (Say, 1829) and other unionid mussels arrived in the Laurentian Great Lakes only after the last glacial maximum in North America. The mussel assemblage is thought to have entered Lake Erie as a wave of expansion from west to east, and moved upstream within tributary rivers. A similar process for most mussels occurred in Lake Ontario, but by eastern species, as the two lake systems are separated by Niagara Falls. Only *P. grandis* is abundant in both lakes. We applied variation in a fragment of the mtDNA Carboxylase I (COI) gene to identify potential historical paths for *P. grandis* to enter these watersheds. Nearly complete monomorphy characterized the Lake Ontario population for the most common Lake Erie allele, which is concordant with sequential founder effects across the Great Lakes. A Φ_{ST} including populations from both Lakes, the intervening Niagara River, tributaries of Lake Erie, and additional samples from below the Laurentian Divide, was 0.10. The southern tributaries of Lake Erie had greater genetic diversity, although few haplotypes were shared among regions or even neighboring streams. Tributary and lake populations differed significantly, yet variation across this divide was not significant. This pattern likely arose from stream capture of upper Ohio River tributaries that once flowed south, and then population isolation, with upstream dispersal from Lake Erie limited to the lower reaches.

INTRODUCTION

Population structure and historical biogeography of freshwater mussels (Unionidae) is often difficult to assess because current populations may be reduced and disjunct (Berg et al., 2007; Zanatta and Harris, 2013), causing many species to be endangered at a state or federal level (Haag and Williams, 2014; Johnson et al., 2018). Common species may therefore be more useful to trace distribution patterns (Mynsberge et al., 2009), especially where genetic markers are applied (Elderkin et al. 2007, 2008; Hewitt et al., 2018; Mathias et al., 2018). Previously, mtDNA sequence data were generated for one such common species, *Pyganodon grandis* (Say, 1829), in Canada (Cyr et al., 2007; Doucet-Beaupré et al., 2012), and across the upper Mississippi watershed and into Lake Erie. Low levels of spatial variation were identified across these once glaciated regions, except for one possible isolated northern glacial refugium in Minnesota that remained unconnected to subsequent colonization of the Great Lakes (Krebs et al. 2015). As *P. grandis* is thought to be a host generalist, this mussel likely followed diverse fishes that spread rapidly into new watersheds (Bernatchez and Wilson, 1998), and it persisted through ecosystem changes that later eliminated or nearly eliminated a great many other species (Zanatta et al., 2015). While *P. grandis* tends to be a small component of mussel assemblages in flowing waters, its ability to colonize small ponds and headwaters (Smith et al., 2002) presents opportunities to move between watersheds

Of the Unionidae, only *P. grandis* is abundant in both lakes Erie and Ontario. Lake Ontario is separated from Lake Erie to the northeast by the 60 km long Niagara River. The lake level falls from 174 m to about 76 m in this short distance with a 70 m drop at Niagara Falls and a series of 5 gorges proceeding down river, forming an effective ecological barrier. The lower elevation coupled with a slight increase in latitude make the regions ecologically similar except that Lake Erie is shallower to the west and Lake Ontario to the east (Bossenbroek et al., 2018; Hoffman et al. 2018). The Appalachian Mountains extend below the lakes forming a sharp front facing east, and the Allegheny Plateau to the west, which form an eastern biogeographic divide. More subtly, a low ridgeline developed just south of Lake Erie, separating the south-flowing Ohio River watershed from the Great Lakes, which all empty north through Lake Ontario and the St. Lawrence Seaway (Lewis et al., 2012). Numerous Lake Erie tributaries possess a diverse yet varied mussel assemblage above a low fall line that forms as the rivers descend the Allegheny Plateau (Lyons et al., 2007), causing upstream (Krebs et al., 2010a, 2013) and near-lake (Crail et al., 2011; Zanatta et al., 2015; Krebs et al., 2018) assemblages to differ. Nonetheless, mixing of various aquatic groups can occur (Rahel, 2007).

We followed up those earlier studies to investigate two knowledge gaps in the genetic structure in *P. grandis* within the Great Lakes: what was the likely source of populations in Lake Ontario on the eastern edge of the St. Lawrence-Great

Lakes biogeographical province (Haag, 2012), and are Lake Erie tributary population related more to the lake populations or to populations in adjacent lotic watersheds. This latter question considers possible historical connectivity between tributaries separated by the Laurentian Divide. Separately, given that an enigmatic and highly divergent (by 9% of nucleotide bases) haplotype form exists within some *P. grandis* populations (Cyr et al., 2007; Doucet-Beaupré et al., 2012), we look at how new data can explain whether these variant haplotypes are of hybrid origin or are historic within the *Pyganodon* lineage and finally touch on how patterns of male-inherited mitochondrial variation contrast with patterns in the classically female-inherited form (Krebs, 2004).

MATERIALS AND METHODS

Over many years, small numbers of individuals, as restricted by permits, were collected across various Ohio streams (Figure 1) initially as whole specimens where *Pyganodon grandis* was common and later just mantle clips during mussel surveys within inlets and river mouths along the southern Great Lakes (Krebs et al., 2010a; Zanatta et al., 2015; Bossenbroek et al., 2018). Here we collated previously published CO1 sequence data from Lake Erie (N=245), regions west of Lake Erie (N=94), and the Niagara River (N=55) (Krebs et al., 2015), and generated new *P. grandis* CO1 sequences (Table 1) from the Lake Ontario region (N=66), Lake Erie tributary streams (N=87), and Ohio River tributary streams (N=20), along with 28 CO1 sequences of the male-inherited mitochondrial lineage.

Total DNA extraction, PCR methods and analyses were described previously for standard female-inherited CO1 barcode sequences and for a small sample of male-inherited sequences that were useful to confirm species identification where female sequences were highly variant

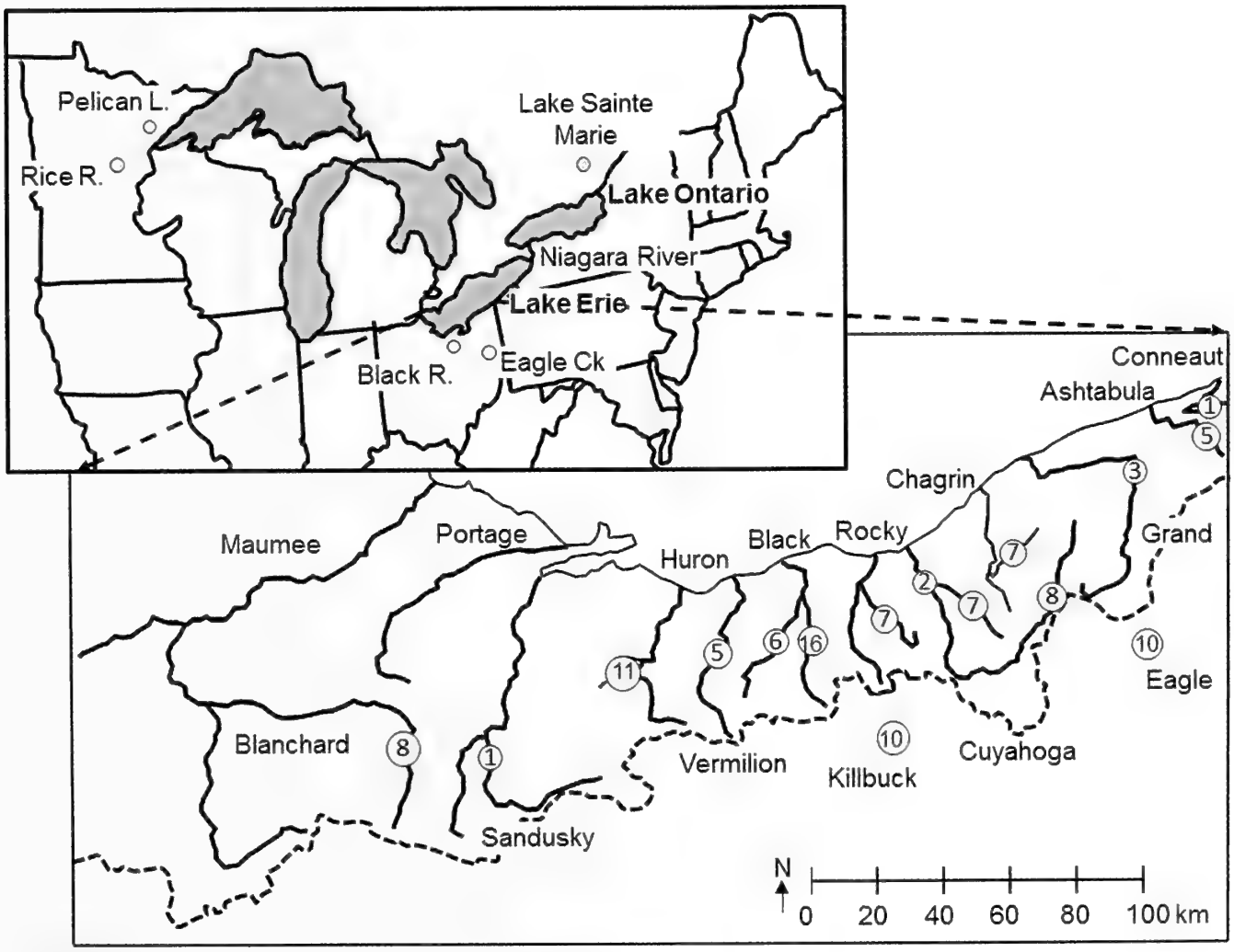

Figure 1. Sampling region of *P. grandis* for the present study, denoting the Great Lakes and five surrounding sites where rare anomalous Type A mitochondrial variants were recovered. The inset shows the rivers sampled with number of individuals sequenced for the various Ohio drainages of Lake Erie, and two additional streams, Eagle and Kilbuck Creeks, which comprise part of the Ohio River headwaters. The Laurentian Divide separating these biogeographic regions is indicated by the dashed line.

Table 1. Genetic diversity in *P. grandis* across the five defined geographic areas, samples from within Lake Erie, the Niagara River, Lake Ontario, the Tributaries of Lake Erie (LE), and for samples from two headwater tributaries of the Ohio River, Eagle Creek and Kilbuck Creek in Ohio. Reported are sample size (N), allele number, polymorphic sites, haplotype diversity (H) or the likelihood that two sequences drawn at random will differ, π, the mean sequence variation among all haplotypes within a population, Θ_s, the estimation of $4N\mu$ based on the number of segregating sites, Θ_π, the estimation of $4N\mu$ based on nucleotide differences, and Tajima's *D*, a test of the difference between Θ_s and Θ_π. which is predicted to be equivalent under neutral evolution.

Region	N	Allele Number	Polymorphic sites	Diversity H	π x 100	Θ_s	Θ_π	Tajima's D
Lake Erie	245	29	31	0.31±0.04	0.085	5.10	0.534	–2.50***
Niagara R.	55	9	8	0.27±0.08	0.057	1.74	0.362	–2.13**
Lake Ontario	66	4	5	0.12±0.05	0.029	1.05	0.181	–1.90**
LE tributaries	87	28	72	0.77±0.05	1.940	14.29	12.22	–0.48
LE tributaries[1]	78	24	22	0.72±0.06	0.186	4.46	1.17	–2.23***
Ohio R. tributaries	20	6	61	0.73±0.07	1.20	17.19	7.579	–2.27***
Ohio R. tributaries[1]	19	5	7	0.70+0.08	0.316	2.00	1.988	–0.02

[1] results omitting the highly variant Type A haplotypes
** $P < 0.01$, *** $P < 0.001$

(Krebs, 2004; Krebs et al., 2015). All haplotype identification codes correspond to the latter paper and Genbank (Table 1). Sequences of individuals were entered into DnaSP V 5.1 from which haplotype networks were constructed in Network V 4.6.1 (Röhl, 2004). Polymorphic sites, transitions, and transversions were weighted equally, although transitions were 6-fold more common and almost every variant was a silent site. A phylogeny was constructed in MEGA7 (v.7.0.26) under maximum likelihood using the Kimura algorithm. The tree topology was exported and drawn in FIGTREE (http://tree.bio.ed.ac.uk/software/figtree/). To contrast biogeographic regions in an Analysis of Molecular Variance (AMOVA), all Lake Erie sequences were pooled, and they were assessed against all samples from Lake Ontario, and all Lake Erie tributary rivers. The samples from below the Laurentian Divide were pooled as a separate group. Among these sets, pairwise Φ_{ST} analyses and a test of neutrality, i.e., Tajima's *D* (Tajima 1989), were run in ARLEQUIN version 3.5.1.2, using 30,000 permutations for tests of significance alone with mismatch analysis as a separate test of population expansion (Excoffier and Lischer, 2010). Tajima's *D* contrasts Θ_s, the estimation of $4N\mu$ based on the number of segregating sites, and Θ_π, the estimation of $4N\mu$ based on nucleotide differences, which are predicted to be the same under neutral evolution and a stable population size.

RESULTS

Expanding the CO1 data set for *P. grandis* to include Lake Ontario, Lake Erie tributaries and two streams south of the Laurentian Divide (Table 1) combined for 31 additional haplotypes based on just a short mtDNA sequence (Figure 2, accession numbers MN125095- MN125125). The Lake Ontario samples were almost monomorphic for the common haplotype, at 94% H1, with only two unique haplotypes collected and one other haplotype that was shared with the Niagara River samples. This common lake haplotype also was the most frequent one in streams, but at a frequency below 50%, making stream samples much more genetically variable than lake samples. For other multicopy haplotypes, most (6 of 8) occurred in only one stream, or only in lake samples (12 of 13 multicopy haplotypes), while only 1 was found both in Lake Erie samples and in a tributary. Similarly, just one haplotype was shared between tributaries separated by the Laurentian Divide.

The extremely high frequency of one allele within the Great Lakes locations produced a small Φ_{ST} (<0.003) between them, but differences between lake and riverine populations led to a pooled $\Phi_{ST} = 0.10$ across all regions. Pairwise Φ_{ST} values (Table 2) produced significant differences between all lake samples and the two pooled river groups, the Lake Erie tributaries and the Ohio River tributaries, while the difference between the two river groups was not significant even though private alleles occurred in several rivers on each side of the divide (Figure 2). The male-inherited form of CO1 showed more sharing of haplotypes (Figure 3, accession numbers MN125131-MN125143) yet they still indicated clear separation between the Black and Cuyahoga rivers, from where most samples derived.

We identified 4 different type A haplotypes among 9 individuals, 8 from the East Branch Black River and 1 from Eagle Creek, albeit a haplotype present in the Black River (Figure 1). Combined with the Type A haplotypes from Doucet-Beaupré et al. (2012), accession numbers MN125127-MN125130, intraspecific variation of 9% at the DNA base level occurs in *P. grandis* (Figure 4). All of these individuals were morphologically identified as *P. grandis*, and sequences of male mitochondria of four of the Black River mussels confirmed their identification. These Type A sequences were similar in distance to the divergence between *P. grandis* and the congeneric species, *P. cataracta* and *P. fragilis*. Adding one type A haplotype available from the Chattahoochee River on the Georgia/Alabama border (Genbank MG199625) and a Type B haplotype from the Escambia River in southern Alabama (Genbank MG199624), supported a hypothesis of basal division between the two haplotype forms. Furthermore, this phylogeny requires the divergence of both forms prior to *P. grandis* migrating north.

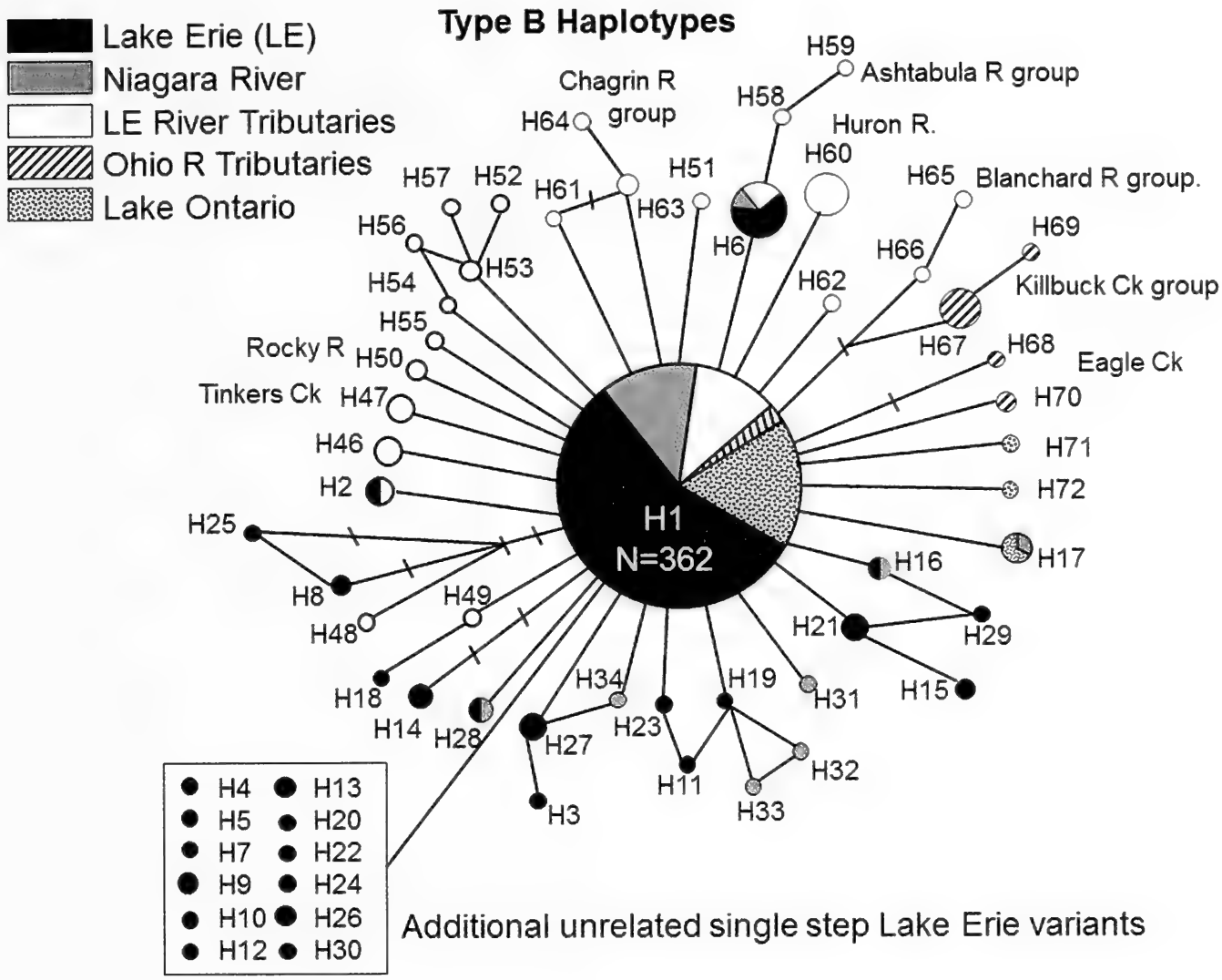

Figure 2. Haplotype network for a fragment of the COI gene amplified in *P. grandis* that were collected across the Lake Erie watershed, Niagara River, Lake Ontario, many tributary streams of Lake Erie, and two streams below the northern divide in the Ohio River watershed. The network reflects the Type B common female mitotype, to which the Type A variant connects distantly (Figure 4). H35–45 occur west and northwest of the Great Lakes and therefore are not included here. Size of the circle reflects the number of that haplotype found. Hatch marks indicate additional mutational steps and labels correspond to the name assigned in Genbank.

To address the process of divergence, Tajima's *D* differed significantly ($\Theta_s >> \Theta_\pi$) in all lake samples (Table 1) as previously reported (Krebs et al., 2015), but results for rivers was confounded by the combined presence of the Type A and Type B forms due to the large number of segregating sites when Type A haplotypes are included. As a consequence, Tajima's D differed significantly in Lake Erie tributaries only when the Type A form was excluded, while the reverse occurred for the Ohio River tributaries. A complementary test, mismatch analysis (in ARLEQUIN

Table 2. Population pairwise Φ_{ST} values among *P. grandis* individuals collected from the 5 regions. Samples derived from within Lake Erie, the Niagara River, Lake Ontario, the Tributaries of Lake Erie, and two headwater tributaries of the Ohio River, Eagle Creek and Kilbuck Creek in Ohio.

Region	Lake Erie	Niagara R.	Lake Ontario	Lake Erie Tributaries
Niagara R.	0.000			
Lake Ontario	0.002	0.002		
Lake Erie Tributaries	0.156***	0.070***	0.080***	
Ohio R. tributaries	0.371***	0.202***	0.241***	0.011

*** P<0.001

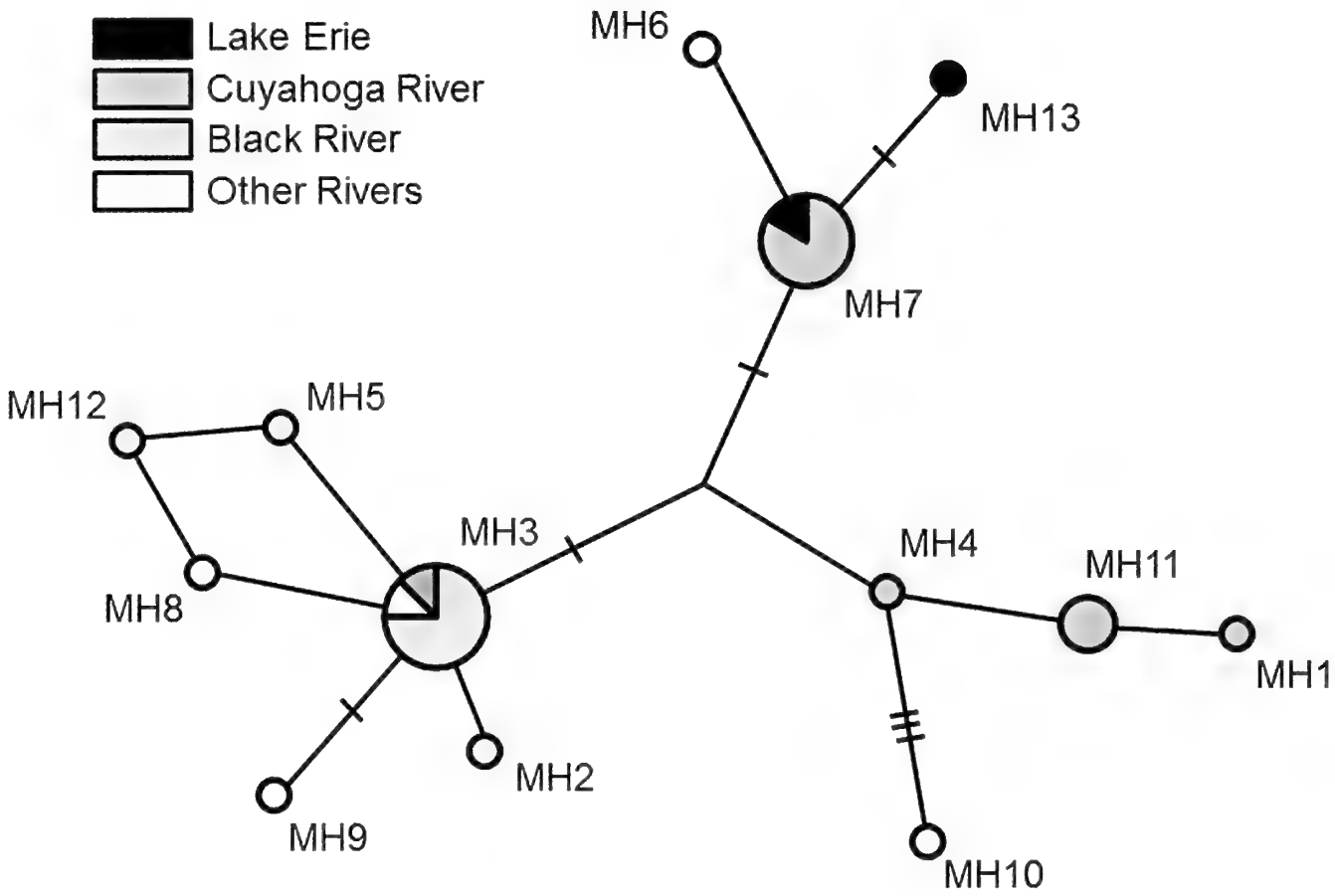

Figure 3. Haplotype network for a fragment of the male-inherited COI gene amplified for a subset (N=28) of the *P. grandis* sampled for population structure. Where multiple allele copies were found, samples came from both above and below the fall lines separating upper and lower reaches. Size of the circle reflects haplotype sample number, with single copies found for all but three. Hatch marks indicate additional mutational steps and labels correspond to the name assigned in Genbank.

and DnaSP), indicated no significant difference from predictions expected under population expansion ($P > 0.05$) in either tributary region or when pooling data for all of the Lake Erie watershed (results not shown).

DISCUSSION

A star pattern of variation in *P. grandis* COI haplotypes (Fig 2) was identified in each region, which infers that one common haplotype is surrounded by many variants of short branch lengths (Avise, 2000; Śmietanka et al., 2009). This pattern is characteristic of populations founded by a small number of individuals that rapidly expanded in size (Braverman et al., 1995). The pattern has persisted even though populations today are much reduced from the past, whether from the invasion of dreissenid mussels depleting and restricting lake populations to coastal areas (Zanatta et al., 2015; Bossenbroek et al., 2018) or where urbanization has depleted habitat in many rivers (Krebs et al., 2010a). Isolation played a concurrent role, shown by a pattern of multiple allele copies or short lineages of related sequences deriving from a single stream.

The evolutionary model that best explains these haplotype patterns in *P. grandis* is one of neutrality where each mutation creates a new allele. Based on this neutral, infinite-allele model, the observed variation in *P. grandis* in Lake Erie suggests that the species exists as one almost panmictic population (Krebs et al., 2015) from which the species expanded into Lake Ontario as a recent colonization wave from a leading edge, which further reduced variation. Today, one haplotype in Lake Erie persists at an allele frequency a little above 80%, rising to over 90% in Lake Ontario. When *P. grandis* may have entered Lake Ontario is unknown. The first Welland Canal connecting lakes Erie and Ontario opened in 1829. But, *P. grandis* also reached the lower Genesee and Oswego basins, the lowland parts of the Mohawk River (Strayer and Jirka, 1997) and the Lake Champlain (Smith 1985) basins of New York State perhaps through links to the Erie Canal that connected the Cuyahoga and Allegheny Rivers, among others (Strayer 1987, 1995). Canals would have provided good habitat for lacustrine species like *P. grandis* (Tevesz et al., 2002a).

Ortmann (1924) proposed that founder events from the west likely produced the mussel assemblage in Lake

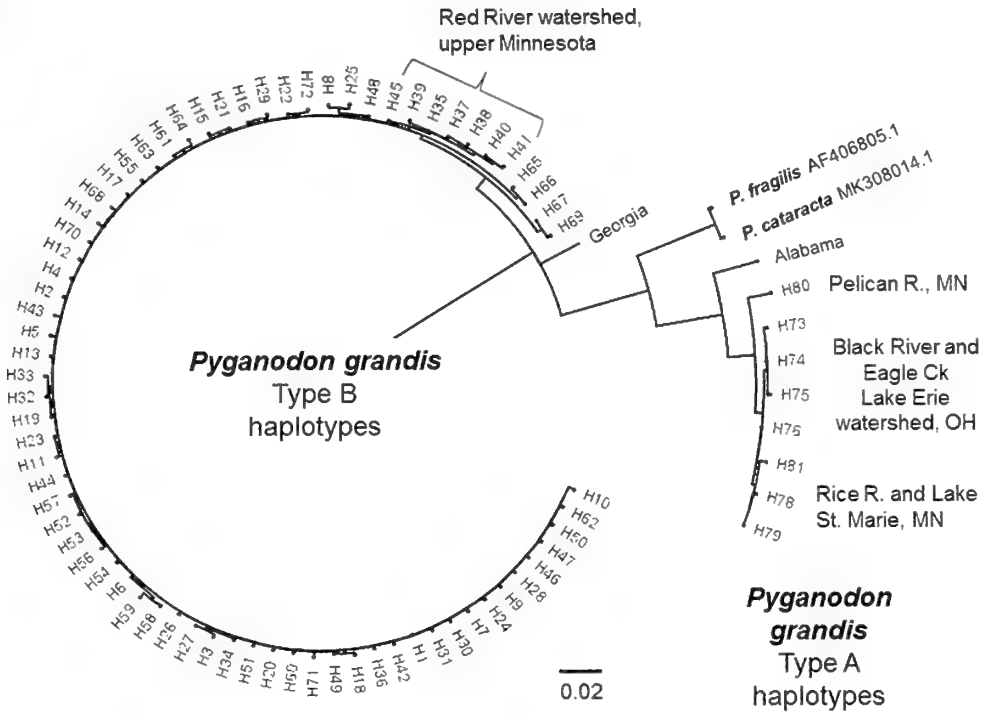

Figure 4. Gene tree for a fragment of the COI gene in *P. grandis* showing the distant relationship between the many Type B haplotypes, and the Type A haplotypes, and haplotypes of two congeneric species that were similarly distant to each haplotype form. Unless indicated, samples span the Midwest and Great Lakes regions. The southern variants fell at the base of each haplotype clade, which supports a deep origin for both haplotype forms predating northern expansion. The Red River clade, which is the most divergent group within the northern samples (Krebs et al., 2015), is highlighted as a contrast to Type A.

Erie, via the Wabash River and its connection to the Maumee watershed, although Graf (2002) expanded the model to multiple lake sources. Little discussion considered river origins for species like *P. grandis*. Variation between Lake Erie populations and those of its tributaries suggests either that mussels independently reached the rivers or that additional colonization events supplemented genetic variation derived from the lake. Assemblages in the Cuyahoga and Black rivers changed over time even before European settlements (Tevesz et al., 2002b), and each river possessed markedly different groups above and below waterfalls that isolated upper reaches (Dean, 1880; Lyons et al, 2007; Krebs et al., 2010b). These rivers descend from a ridge line at about 300 m down to Lake Erie at 175 m, and at least one high waterfall formed in each river. In another locally common mussel, *Lampsilis siliquoidea* (Barnes, 1823), the impact of these falls among neighboring streams was visible in large differences in female-inherited haplotype frequencies, while the same male-inherited sequences could be found above and below waterfalls (Krebs et al., 2013).

Movement across watersheds probably involved headwater capture following glacial retreat and isostatic rebounding, a process that is well documented across the Great Lakes watershed subsequent to the last glaciers, 12000–15000 years ago (Coffey, 1958; Bishop, 1995). By that time, populations of *P. grandis* had likely expanded in the upper Ohio River south of the glacial line providing more time for new mutations to arise from a common haplotype. Simple mutation-drift dynamics could create the presently observed patterns in genetic variation, requiring only typical mitochondrial mutation rates (Haag-Liautard et al., 2008; Hamilton, 2009) and modest historical effective population sizes, which are a reasonable expectation for this generalist species (Watters et al., 2009). Partitioned sub-populations would enable drift to randomly impact isolated alleles (Wright, 1931, 1932), and do so differently among streams, to which additional mutation and occasional migration can be added (Hössjer et al., 2014). Thus, the post-glacial time period for the region likely sufficed for both rare variants to arise and a common allele to slowly decline following sequential colonization sweeps, with related but different rare haplotypes arising in streams.

Genetically unusual if not unique for *P. grandis* is the co-occurrence of two highly differentiated (9%) mtDNA forms. Support for ancient divergence within *P. grandis* over some form of introgression derives from the phylogeny (Fig 4.) that includes one Type A haplotype from the Chattahoochee River on the Georgia/Alabama border (Genbank Accession MG199625), and a Type B haplotype came from the Escambia River in southern Alabama (Genbank MG199624) (Smith et al., 2018 a, b). A BLAST search showed each sequence to be only 96-97% similar to their respective northern clade relatives, while all northern sequences within both clades were much more closely related to each other at 1–2%. Therefore, Type A

and Type B mitochondrial types have likely co-occurred in *P. grandis* a very long time, possibly since before the radiation of the genus, and both haplotypes were carried northward in migrants following glacial retreat. Other haplotypes likely came too, and they reached across headwaters where simple drift processes limited what haplotypes remain today.

In sum, the historical movement of *P. grandis* demonstrates how population structure may have arisen in many mussels, arriving through different channels from the south in the Pleistocene. *Pyganodon grandis* was just more extreme in its success, as it reached across to eastern Colorado (Liu et al., 1996), up the Mississippi to northern Minnesota (Krebs et al., 2015) and Canada (Doucet-Beaupré et al., 2012), and separately, along the Ohio River and Wabash River to reach the lakes and through eastern tributaries to access streams below the lakes. It has even dispersed to the Escambia-Choctawhatchee watersheds (Haag, 2012) and south to Mesoamerica (Pfeiffer et al., 2019), probably long before any colonization of the Great Lakes. Perhaps these areas were reached when sea levels were low and glaciers high (Swift et al., 1986). Yet, the large lacustrine populations became the least genetically diverse, probably from rapid and sequential population expansion, a process that favors few or one allele compared to the expectations with stream capture of already diverse populations.

ACKNOWLEDGMENTS

Collections in the Great Lakes were funded by the U.S. Fish and Wildlife Service – Great Lakes Fish and Wildlife Restoration Act (#30181AG152). Other financial support included a Research Experiences for Undergraduates award from the National Science Foundation (DBI 0243878), and M. Lyons, who initiated the tributary work, was supported by a National Oceanic and Atmospheric Administration fellowship (NA07-NOS4200018), while RAK was supported by an Established Full-time Faculty Research and Development award from Cleveland State University. Scientific collection permits were provided by wildlife agencies of Ohio, New York, and Ontario. Many helped provide specimens for this study over the years, A. Karatayev, B. Tulumello and K. Bauer (SUNY Buffalo State College) plus Wendy Paterson, Traci Griffith, Mariah Scott, Ethan Nederhoed, Lindsey Kolich, and Emily Marlow (CMU) all assisted in sampling in New York, while Paul Doerder, Louie Rundo, Dan Gouch, Mark Lyons, Jeremy Holt, John Hook, David Kriska, Jeff Pallotta, and Erin Steiner helped collect in various tributary streams, and Mark Lyons, Matt Begley and Nikko Hogya helped with DNA processing. We thank John Pfeiffer and Kevin Cummings for many constructive suggestions during review. This article is contribution #132 of the Central Michigan University Institute for Great Lakes Research.

LITERATURE CITED

Avise, J.C. 2000. Phylogeography: The History and Formation of Species. Harvard University Press, Cambridge, Massachusetts.

Berg, D.J., A.D. Christian, and S.I. Guttman. 2007. Population genetic structure of three freshwater mussel (Unionidae) species within a small stream system: significant variation at local spatial scales. Freshwater Biology 52: 1427–1439.

Bernatchez, L. and C.C. Wilson, 1998. Comparative phylogeography of Nearctic and Palearctic fishes. Molecular Ecology 7: 431–452.

Bishop, P. 1995. Drainage rearrangement by river capture, beheading and diversion. Progress in Physical Geography 19: 449–473.

Bossenbroek, J.M., L.E. Burlakova, T.C. Crail, A.Y. Karatayev, R.A. Krebs, and D.T. Zanatta. 2018. Modelling habitat of freshwater mussels (Bivalvia: Unionidae) in the lower Great Lakes 25 years after the *Dreissena* invasion. Freshwater Science 37: 330–342.

Braverman, J.M., R.R. Hudson, N.L. Kaplan, C.H. Langley, and W. Stephan. 1995. The hitchhiking effect on the site-frequency spectrum of DNA polymorphisms. Genetics 140: 783–796.

Crail, T.D., R.A. Krebs, and D.T. Zanatta. 2011. Unionid mussels from nearshore zones of Lake Erie. Journal of Great Lakes Research 37: 199–202.

Coffey, G.N. 1958. Major glacial drainage changes in Ohio. Ohio Journal of Science 58: 43–49.

Cyr, F., A. Paquet, A.L. Martel, and B. Angers. 2007. Cryptic lineages and hybridization in freshwater mussels of the genus *Pyganodon* (Unionidae) in northeastern North America. Canadian Journal of Zoology 85: 1216–1227.

Dean, G.W. 1890. Distribution of Unionidae in the three rivers Mahoning, Cuyahoga and Tuscarawas. Nautilus 4: 20–22.

Doucet-Beaupré, H., P.U. Blier, E.G. Chapman, H. Piontkivska, F. Dufresne, B.E. Sietman, R.S. Mulcrone, and W.R. Hoeh. 2012. *Pyganodon* (Bivalvia: Unionoida: Unionidae) phylogenetics: A male- and female-transmitted mitochondrial DNA perspective. Molecular Phylogenetics and Evolution 63: 430–444.

Elderkin, C.L., A.D. Christian, C.C. Vaughn, J.L. Metcalfe-Smith, and D.J. Berg. 2007. Population genetics of the freshwater mussel, *Amblema plicata* (Say 1817) (Bivalvia: Unionidae): Evidence of high dispersal and post-glacial colonization. Conservation Genetics 8: 355–372

Elderkin, C.L., A.D. Christian, J.L. Metcalfe-Smith, and D.J. Berg. 2008. Population genetics and phylogeography of freshwater mussels in North America, *Elliptio dilatata* and *Actinonaias ligamentina* (Bivalvia: Unionidae). Molecular Ecology 17: 2149–2163.

Excoffier, L. and H.E.L. Lischer. 2010. Arlequin suite ver 3.5: A new series of programs to perform population genetics analyses under Linux and Windows. Molecular Ecology Resources 10: 564–567.

Graf, D.L. 2002. Historical biogeography and late glacial origin of the freshwater pearly mussel (Bivalvia: Unionidae) faunas of Lake Erie. North American Museum of Comparative Zoology, Occasional Papers on Molluscs 6: 175–210.

Haag, W.R. 2012. North American Freshwater Mussels: Natural History, Ecology, and Conservation. Cambridge University Press, New York.

Haag, W.R. and J.D. Williams. 2014. Biodiversity on the brink: an assessment of conservation strategies for North American freshwater mussels. Hydrobiologia 735: 45–60.

Haag-Liautard, C., N. Coffey, D. Houle, M. Lynch, B. Charlesworth, and P.D. Keightley. 2008. Direct estimation of the

mitochondrial DNA mutation rate in *Drosophila melanogaster*. PLoS Biology 6(8):e204.
Hamilton, M.B. 2009. Population Genetics. Wiley-Blackwell. West Sussex, U.K.
Hewitt, T.L. J.L. Bergner, D.A. Woolnough, and D.T. Zanatta. 2018. Phylogeography of the freshwater mussel species *Lasmigona costata*: Testing post-glacial colonization hypotheses. Hydrobiologia 810: 191–206.
Hoffman, J.R., T.J. Morris, and D.T. Zanatta. 2018. Genetic evidence for canal-mediated dispersal of Mapleleaf (*Quadrula quadrula*, Bivalvia: Unionidae) on the Niagara Peninsula, Canada. Freshwater Science 37: 82–95.
Hössjer, O., F. Olsson, L. Laikre, and N. Ryman. 2014. A new general analytical approach for modeling patterns of genetic differentiation and effective size of subdivided populations over time. Mathematical Biosciences 258: 113–133.
Johnson, N.A., C.H. Smith, J.M. Pfeiffer, C.R. Randklev, J.D. Williams, and J.D. Austin. 2018. Integrative taxonomy resolves taxonomic uncertainty for freshwater mussels being considered for protection under the US Endangered Species Act. Scientific reports 8(1): 15892.
Krebs, R.A. 2004. Combining paternally and maternally inherited mitochondrial DNA for analysis of population structure in mussels. Molecular Ecology 13: 1701–1705.
Krebs, R.A., W.C. Borden, E.R. Steiner, M.S. Lyons, W. Zawiski, and B.M. Walton. 2010a. Determinants of mussel diversity in Lake Erie tributaries. Journal of the North American Benthological Society 29: 506–520.
Krebs, R.A., J.D. Hook, M.A. Hoggarth, and B.M. Walton. 2010b. Evaluating the mussel fauna of the Chagrin River, A state listed "scenic" river in Ohio. Northeastern Naturalist 17: 565–574.
Krebs, R.A., W.C. Borden, N.M. Evans, and F.P. Doerder. 2013. Differences in population structure between maternally- and paternally-inherited forms of mitochondria in *Lampsilis siliquoidea* (Bivalvia: Unionidae). Biological Journal of the Linnean Society 109: 229–240.
Krebs, R.A., B.D. Allen, N.M. Evans, and D.T. Zanatta. 2015. Mitochondrial DNA structure of *Pyganodon grandis* (Bivalvia: Unionidae) from the Lake Erie watershed and selected locations in its northern distribution. American Malacological Bulletin 33: 5–13.
Krebs, R.A., T.J. Prescott, W.B. Clapham, and D.A. Klarer. 2018. Freshwater mussel assemblages at the lotic-lentic interface along Lake Erie. American Malacological Bulletin 36: 31–41.
Lewis, C.F.M., G.D.M. Cameron, T.W. Anderson, C.W. Heil Jr., and P.L. Gareau. 2012. Lake levels in the Erie Basin of the Laurentian Great Lakes. Journal of Paleolimnology 47: 493–511.
Liu, H.P., J.B. Mitton, and S.J. Herrmann. 1996. Genetic differentiation in and management recommendations for the freshwater mussel, *Pyganodon grandis* (Say, 1829). American Malacological Bulletin 13: 117–124.
Lyons, M.S., R.A. Krebs, J.P., Holt, L.J Rundo, and W. Zawiski. 2007. Assessing causes of change in the freshwater mussels (Bivalvia: Unionidae) in the Black River, Ohio. American Midland Naturalist 158: 1–15.
Mathias, P.T., J.R. Hoffman, C.C. Wilson, and D.T. Zanatta. 2018. Signature of postglacial colonization on contemporary genetic structure and diversity of *Quadrula quadrula* (Bivalvia: Unionidae). Hydrobiologia 810: 207–225.
Mynsberge, A.R., M.P. Strager, J.M. Strager, and P.M. Mazik. 2009. Developing predictive models for freshwater mussels (Mollusca: Unionidae) in the Appalachians: Limitations and directions for future research. Ecoscience 16: 387–398.
Ortmann, A.E. 1924. Distributional features of naiades in tributaries of Lake Erie. American Midland Naturalist 9: 101–117.
Pfeiffer, J.M., C.L. Atkinson, A.E. Sharpe, K.A. Capps, K.F. Emery, and L.M. Page. 2019. Phylogeny of Mesoamerican freshwater mussels and a revised tribe-level classification of the Ambleminae. Zoologica Scripta, 48: 106–117.
Rahel, F.J. 2007. Biogeographic barriers, connectivity and homogenization of freshwater faunas: it's a small world after all. Freshwater Biology 52: 696–710.
Röhl, A. 2004. NETWORK version 4.5.1.0. Shareware phylogenetic network software presented by Fluxus Technology Ltd. Available at http://www.fluxus-engineering.com. April 2013.
Śmietanka, B., A. Burzyński, and R. Wenne. 2009. Molecular population genetics of male and female mitochondrial genomes in European mussels *Mytilus*. Marine Biology 156: 913–925.
Smith, C.H., N.A. Johnson, J.M. Pfeiffer, and M.M. Gangloff. 2018a. Molecular and morphological data to facilitate future research on freshwater mussels (Bivalvia: Unionidae: Anodontinae). Data in Brief 17: 95–104.
Smith, C.H., N.A. Johnson, J.M. Pfeiffer, and M.M. Gangloff. 2018b. Molecular and morphological data reveal non-monophyly and speciation in imperiled freshwater mussels (*Anodontoides* and *Strophitus*). Molecular Phylogenetics and Evolution 119: 50–62.
Smith, D.C., M.A. Gates, R.A. Krebs, and M.J.S. Tevesz. 2002. A survey of freshwater mussels (Unionidae) and other molluscs in the Cuyahoga Valley National Park. Ohio Biological Survey, Miscellaneous Contribution No. 8: iv–31p.
Smith, D.G. 1985. A study of the distribution of freshwater mussels (Mollusca: Pelecypoda: Unionoida) of the Lake Champlain drainage in northwestern New England. American Midland Naturalist 114: 19–29.
Strayer, D.L. 1987. Ecology and zoogeography of the freshwater mollusks of the Hudson River basin. Malacological Review 20: 1–68.
Strayer, D.L. 1995. Some collections of freshwater mussels from Schoharie Creek, Tonawanda Creek, and the Allegheny basin in New York in 1994. Report to the New York Natural Heritage Program, Latham, NY. 3 pp.
Strayer, D.L. and K.J. Jirka. 1997. The Pearly Mussels of New York State. New York State Museum Memoir 26. State Education Department, Albany, New York.
Swift, C.C, C.R. Gilbert, S.A. Bortone, G.H. Burgess, and R.W. Yerger. 1986. The zoogeography of the freshwater fishes of the Southeastern United States: Savannah River to Lake Pontchartrain. In Hocutt, C.H. and E.O. Wiley, (eds.) The Zoogeography of North American freshwater fishes. John Wiley, New York. pp. 213–265.
Tajima, F. 1989. Statistical method for testing the neutral mutation hypothesis by DNA polymorphism. Genetics 123: 585–595.
Tevesz, M.J.S., L. Rundo, and R.A. Krebs. 2002a. Freshwater mussels (Bivalvia: Unionidae) of the Ohio & Erie Canal, Cuyahoga Valley National Park, Ohio. Kirtlandia 53: 35–36.
Tevesz, M.J.S., L. Rundo, R.A. Krebs, B.G. Redman, and A.S. DuFresne. 2002b. Changes in the freshwater mussel (Bivalvia: Unionidae) fauna of the Cuyahoga River, Ohio, since late prehistory. Kirtlandia 53: 13–18.
Watters, G.T., M.A. Hoggarth, and D.H. Stansbery. 2009. The Freshwater Mussels of Ohio. The Ohio State University Press, Columbus, Ohio.
Wright, S. 1931. Evolution in Mendelian populations. Genetics 16: 97–159.

Wright, S. 1932. The roles of mutation inbreeding and crossbreeding and selection in evolution. Proceedings of the Sixth International Congress of Genetics 1: 356–366.

Zanatta, D.T. and A.T. Harris. 2013. Phylogeography and genetic variability of the freshwater mussels (Bivalvia: Unionidae) Ellipse, *Venustaconcha ellipsiformis* (Conrad 1836), and Bleeding Tooth, *V. pleasii* (Marsh 1891). American Malacological Bulletin 31: 267–279.

Zanatta, D.T., J. Bossenbroek, L.E. Burlakova, T. Crail, F. de Szalay, T.A. Griffith, D. Kapusinski, A.Y. Karatayev, R.A. Krebs, E.S. Meyer, W.L. Paterson, T.J. Prescott, M.T. Rowe, D.W. Schloesser, and M.C. Walsh. 2015. Distribution of native mussel (Unionidae) assemblages in coastal Lake Erie, Lake St. Clair, and Connecting Channels, twenty-five years after a dreissenid invasion. Northeastern Naturalist 22: 223–235.

Appendix 1. Supplemental Table. The samples used in the present study labeled by haplotype number. The main biogeographic region is provided relevant to previous work (Krebs et al., 2015) with new samples for Lake Ontario, Lake Erie (LE) tributary rivers and two rivers from south of the Laurentian Divide, Kilbuck and Eagle Creeks, which are in the Ohio River watershed. Subwatersheds list the specific area of collection along with sample size (N), Genbank accession numbers, and a pair of coordinates within the range of that haplotype.

Haplo-type	Region	Sub watershed	N	Accession #	Latitude	Longitude
H1	All regions except Red River	most if not all sub-watersheds	416	KM262507.1		
H2	LE & Tributary	Sheldon Marsh, Vermilion River	2	KM262508.1	41.4246	–82.6242
H3	Lake Erie	Sheldon Marsh	1	KM262509.1	41.4246	–82.6242
H4	LE & Sandusky Bay	Old Woman Creek, Yellow Swale	2	KM262510.1	41.3794	–82.5117
H5	Lake Erie	Old Woman Creek	1	KM262511.1	41.3794	–82.51173
H6	LE, Niagara R. & Tributaries	Many nearshore sites & Ashtabula River	8	KM262512.1	41.8582	–80.6397
H7	Sandusky Bay	South Creek	1	KM262513.1	41.398	–83.0106
H8	Sandusky Bay	South Creek, Yellow Swale	2	KM262514.1	41.398	–83.0106
H9	Sandusky Bay	Muddy Creek Bay	1	KM262515.1	41.4496	–83.0281
H10	Lake Erie	Plum Brook	1	KM262516.1	41.4247	–82.639
H11	Lake Erie	Cranberry Creek	1	KM262517.1	41.3824	–82.4727
H12	Lake Erie	Cranberry Creek	1	KM262518.1	41.3824	–82.4727
H13	Lake Erie	Crane Creek	2	KM262519.1	41.6275	–83.2018
H14	Lake Erie & Sandusky Bay	Turtle Creek	3	KM262520.1	41.6031	–83.1517
H15	Lake Erie	Turtle Creek	2	KM262521.1	41.6031	–83.1517
H16	Sandusky Bay & Niagara R.	Grand Isle & Muddy Creek Bay	2	KM262522.1	43.0395	–78.8937
H17	Niagara River & Lake Ontario	Grand Isle & Eastern inlets	3	KM262523.1	43.6254	–76.1959
H18	Lake Erie	Misery Bay	1	KM262524.1	42.1614	–80.0898
H19	Lake Erie	Duck Pond	1	KM262525.1	42.0956	–80.071
H20	Lake Erie	Misery Bay	1	KM262526.1	42.1614	–80.0898
H21	Lakes Erie & St Clair	East Harbor, Young Marsh	3	KM262527.1	41.5421	–82.8104
H22	Lake Erie	Crane Creek	1	KM262528.1	41.6275	–83.2017
H23	Sandusky Bay	Muddy Creek Bay	1	KM262529.1	41.4496	–83.0281
H24	Sandusky Bay	Muddy Creek Bay	1	KM262530.1	41.4496	–83.0281
H25	Lake Erie	East Harbor	1	KM262531.1	41.5421	–82.8104
H26	Lake Erie	North Maumee Bay, Turtle Creek	2	KM262532.1	45.9184	–89.5324
H27	Lake Erie	Toussiant Creek	2	KM262533.1	41.5784	–83.1085
H28	Lake Erie and Niagara R.	Turtle Creek, Strawberry Island	2	KM262534.1	41.6031	–83.1517
H29	Lake Erie	Turtle Creek	1	KM262535.1	41.6031	–83.1517
H30	Lake Erie	Turtle Creek	1	KM262536.1	41.6031	–83.1517
H31	Niagara River	Strawberry Island	1	KM262537.1	42.9539	–78.9235
H32	Niagara River	Strawberry Island	1	KM262538.1	42.9539	–78.9235
H33	Niagara River	Strawberry Island	1	KM262539.1	42.9539	–78.9235
H34	Niagara River	Strawberry Island	1	KM262540.1	42.9539	–78.9235
H35	Minnesota (NW)	Red River and upper lakes, Minnesota.	8	KM262541.1	47.8253	–93.3748
H36	Minnesota	Lac Qui R.; lower Minn R., Minn.	3	KM262542.1	45.0166	–95.8866
H37	Minnesota (NW)	Rice R., Deer L. Upper Minnesota	6	KM262543.1	46.5326	–93.32
H38	Minnesota (NW)	Pfeiffer Lake, Upper Minnesota	4	KM262544.1	47.7515	–92.4771
H39	Minnesota (NW)	Pfeiffer Lake, Upper Minnesota	1	KM262545.1	47.8253	–93.3748
H40	Minnesota (NW)	Prairie River, Upper Minnesota	12	KM262546.1	47.2391	–93.4821
H41	Minnesota (NW)	Prairie River, Upper Minnesota	1	KM262547.1	47.2391	–93.4821
H42	Minnesota (NW)	Prairie Lake, Michigan	2	KM262548.1	41.8586	–85.4037
H43	Minnesota (NW)	Big Fork R., Upper Minnesota	1	KM262549.1	47.8004	–93.5724
H44	Upper Great Lakes	North Twin Lake, WI	1	KM262550.1	46.0665	–89.0887
H45	Upper Great Lakes	Annabelle & St. Germaine Lakes, WI	2	KM262551.1	46.2206	–89.6787
H46	LE Tributary	Black, Grand, Cuyahoga (above falls) Rivers	3	MN125095	41.4545	–82.1354
H47	LE Tributary	Cuyahoga River (Tinkers Creek, above falls)	3	MN125096	41.3146	–81.4354
H48	LE Tributary	Cuyahoga River (Tinkers Creek, above falls)	1	MN125097	41.3146	–81.4354
H49	LE Tributary	Cuyahoga River (Tinkers Creek, above falls)	1	MN125098	41.3146	–81.4354
H50	LE Tributary	Cuyahoga River (Tinkers Creek, above falls)	2	MN125099	41.3146	–81.4354
H51	LE Tributary	Black River	1	MN125100	41.4545	–82.1354
H52	LE Tributary	Black River	1	MN125101	41.4545	–82.1354
H53	LE Tributary	Black River, Cuyahoga River (above falls)	2	MN125102	41.4545	–82.1354

(*Continued*)

Appendix 1. (Continued)

Haplo-type	Region	Sub watershed	N	Accession #	Latitude	Longitude
H54	LE Tributary	Black River West Branch	1	MN125103	41.3141	–82.1316
H55	LE Tributary	Cuyahoga River (above falls)	1	MN125104	41.3018	–81.2026
H56	LE Tributary	Cuyahoga River (above falls)	1	MN125105	41.3018	–81.2026
H57	LE Tributary	Ashtabula River East Branch	1	MN125106	41.8119	–80.5973
H58	LE Tributary	Ashtabula River East Branch	1	MN125107	41.8119	–80.5973
H59	LE Tributary	Ashtabula River West Branch	1	MN125108	41.7645	–80.6155
H60	LE Tributary	Huron River West Branch	7	MN125109	41.286	–82.6435
H61	LE Tributary	Rocky River East Branch (drained pond)	1	MN125110	41.2445	–81.6779
H62	LE Tributary	Rocky River East Branch (drained pond)	1	MN125111	41.2445	–81.6779
H63	LE Tributary	Chagrin River (above falls)	2	MN125112	41.5257	–81.2605
H64	LE Tributary	Chagrin River (above falls)	1	MN125113	41.5257	–81.2605
H65	LE Tributary	Blanchard River	1	MN125114	40.8915	–83.5643
H66	LE Tributary	Blanchard River	1	MN125115	40.8915	–83.5643
H67	Ohio River Tributary	Killbuck Creek	6	MN125116	40.9528	–82.0262
H68	Ohio River Tributary	Killbuck Creek	1	MN125117	40.9528	–82.0262
H69	Ohio River Tributary	Killbuck Creek	1	MN125118	40.9528	–82.0262
H70	Ohio River Tributary	Eagle Creek (Mahoning R. watershed)	1	MN125119	41.2827	–81.118
H71	Lake Ontario	Blind Sodus Bay	1	MN125120	43.338	–76.7281
H72	Lake Ontario	North Bay	1	MN125121	43.6314	–76.1919
H73	LE Tributary	Black River East Branch	1	MN125122	41.2363	–82.0797
H74	LE Tributary	Black River East Branch	6	MN125123	41.2363	–82.0797
H75	LE Tributary	Black River East Branch	1	MN125124	41.2363	–82.0797
H76	LE & Ohio R. Tributary	Black River East Branch, Eagle Creek	2	MN125125	41.2363	–82.0797
H78	Quebec, Canada	Lac Sainte Marie	1	MN125127	45.9561	–75.9305
H79	Quebec, Canada	Lac Sainte Marie	1	MN125128	45.9561	–75.9305
H80	Minnesota (NW)	Pelican Lake Minnesota	2	MN125129	48.0633	–92.8321
H81	Minnesota (NW)	Rice River	3	MN125130	46.5326	–93.32
MH1	LE Tributary	Cuyahoga River (above falls)	1	MN125131	41.3018	–81.2026
MH2	LE Tributary	Black River	1	MN125132	41.45453	–82.1354
MH3	LE Tributaries	Black River West Branch, Tinkers Creek, Ashtabula River	8	MN125133	41.2951	–82.1486
MH4	LE Tributary	Cuyahoga River (Tinkers Creek, above falls)	1	MN125134	41.3146	–81.4354
MH5	LE Tributary	Black River	1	MN125135	41.45453	–82.1354
MH6	LE Tributary	Conneaut Creek	1	MN125136	41.9041	–80.5289
MH7	LE Tributaries	Diverse Rivers, Sandusky Bay	7	MN125137	41.4195	–82.9227
MH8	LE Tributary	Black River East Branch	1	MN125138	41.2363	–82.0797
MH9	LE Tributary	Huron River west branch	1	MN125139	41.286	–82.6435
MH10	LE Tributary	Huron River west branch	1	MN125140	41.286	–82.6435
MH11	LE Tributary	Cuyahoga River & Tinkers Creek (above falls)	3	MN125141	41.3018	–81.2026
MH12	LE Tributary	Black River East Branch	1	MN125142	41.2363	–82.0797
MH13	Lake Erie	Sandusky Bay	1	MN125143	41.4195	–82.9227

Description of two new muricid species (Gastropoda: Muricidae: Muricopsinae) from the western Atlantic and the eastern Pacific

Roland Houart
Institut royal des Sciences naturelles de Belgique[1]
and
Muséum national d'Histoire naturelle, Paris, France[2]
UMR7205 ISyEB
roland.houart@skynet.be

ABSTRACT

Two new species of Muricidae are described from Brazil and from the Pacific coast of Panama. *Favartia aquinoi* new species from Brazil is compared with the related *F. glypta* (M. Smith, 1938), as well as with *F. cellulosa* (Conrad, 1846) and *F. levicula* (Dall, 1889). *Muricopsis vassarti* new species is described from the Pacific coast of Panama and compared with three other *Muricopsis* species from the Eastern Pacific, *M. zeteki* Hertlein and Strong, 1951, *M. westonensis* Myers and D'Attilio, 1990 and *M. taupini* Garrigues, 2016.

Additional Keywords: Favartia, *Muricopsis* new species, Brazil, Panama, eastern Pacific

INTRODUCTION

Muricopsinae comprise 13 genera and one subgenus [*Muricopsis* (*Risomurex*)] and include some 268 species (Houart, 2018, updated). Two new species are described herein, the first, from Brazil, is assigned to *Favartia* Jousseaume, 1880, the second is a *Muricopsis* s.s. species from Pacific Panama.

Thirty Recent species are assigned to the genus *Favartia* in the Western Atlantic (MolluscaBase 2019a). This number includes species of *Favartia* (*Murexiella*) and may slightly differ in recent publications, depending on what synonyms are considered by the authors.

A group of species is of particular interest. It is composed of *F. glypta* (M. Smith, 1938), *F. cellulosa* (Conrad, 1846), *F. levicula* (Dall, 1889) and a new species described from Brazil.

Rios (1985) considered *Murexiella iemanja* Petuch, 1979, described from the Abrolhos Archipelago in Brazil, a synonym of *F. glypta* from the Pliocene of Clewiston, Florida, but also known from the Recent fauna and occurring in several places from Florida to Brazil. He was followed by Houart (1991: 32) and by Vokes (1994: 112).

Favartia glypta was considered a synonym of *F. levicula* by Radwin and D'Attilio (1976: 159). However, these two species differ in shell ornamentation and protoconch characters. The protoconch of *F. glypta* is paucispiral, consisting of 1.5 rounded whorls (Figures 3, 25) while that of *F. levicula* is conical and multispiral, consisting of almost 4 whorls (Figure 37).

The Western Atlantic and Eastern Pacific species assigned to *Muricopsis* by several authors, such as Keen (1971), Vokes (1971, 1994), Kaicher (1974, 1978, 1980, 1991), Fair (1976), Radwin and D'Attilio (1976) and many others are now assigned to *Muricopsis* and to *Murexsul* (MolluscaBase, 2019b), depending on their shell morphology (Merle and Houart, 2003).

The species of *Muricopsis* are characterized by the hypertrophy of apertural denticle D2 and by strong columellar folds. The spiral sculpture consists of primary cords P1–P5 on the convex part of the teleoconch whorl, atrophied P6 on the siphonal canal, followed by primary cords ADP and occasionally MP. In *Murexsul oxytata* (M. Smith, 1938) and other species of that group, the P2 primary cord is atrophied and the columellar folds are absent.

Of the four Eastern Pacific species that had been included in *Muricopsis*, two remain in *Muricopsis*: *M. pauxilla* (A. Adams, 1854) and *M. zeteki* Hertlein and Strong, 1951, and two have been reassigned to *Murexsul*: *M. armatus* (A. Adams, 1854) and *M. jaliscoensis* (Radwin and D'Attilio, 1970). While the spiral sculpture of *M. pauxilla* is typical for *Muricopsis*, it lacks columellar folds. Two additional species of *Muricopsis* were subsequently described, *M. westonensis* Myers and D'Attilio, 1990, from Cocos Island, Costa Rica and *M. taupini* Garrigues, 2016, from the Galapagos. A fifth species of *Muricopsis*, syntopic with *M. zeteki*, is here described as new.

A broad phylogenetic analysis of Muricopsinae is needed in order to verify the status of some genera and assigned species.

[1] Research Associate
[2] Research Associate

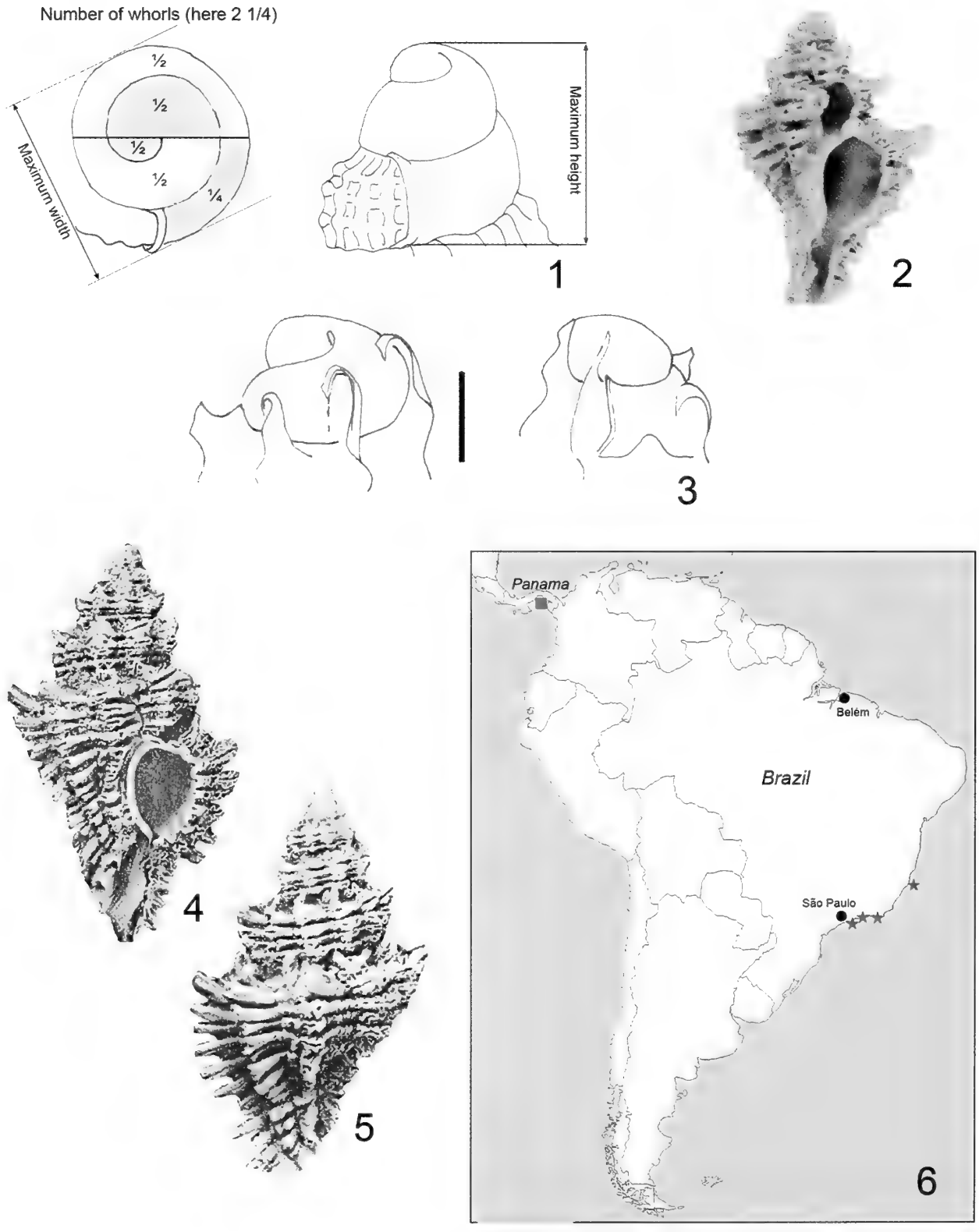

Figures 1–6. Two new species of Muricopsinae. **1.** Method for determining diameter, height and counting the number of protoconch whorls. **2–5.** *Favartia glypta* (M. Smith, 1938). **2.** Paratype of *Murexiella iemanja* Petuch, 1979. Brazil, Bahia State, 2 km E Santa Bárbara Island, Abrolhos Archipelago, Chapeirão Reef, 25 m, USNM 780653. **3.** Protoconch of *Murexiella iemanja* Petuch, 1979, holotype USNM 780652. **4–5.** Florida, Hendry County, Clewiston, Caloosahatchee Formation, Pliocene, Holotype, University of Alabama, Museum of Natural History, 25.3 mm (reproduced from Vokes, 1968). **6.** Distribution of *Favartia aquinoi* new species (red stars) and *Muricopsis (Muricopsis) vassarti* new species (red square). Scale bar = 500 μm.

MATERIALS AND METHODS

The new material studied was collected between 1960 and 2008 in Pacific Panama and along the Brazilian coast. The material used for comparison is deposited in MNHN, USNM and in the author's private collection.

Characters used to describe shell morphology address the general aspect of the shell, its shape, size, and color, the shape of the spire including the protoconch, the number and features of the teleoconch whorls, details of the suture and of the subsutural ramp, details of axial and spiral sculpture, the aperture, the siphonal canal and the operculum. The description is based on the type material.

The method used to determine diameter and height, and to count the number of protoconch whorls, follows Bouchet and Kantor (2004) as shown in Figure 1.

Abbreviations used in the text are as follows: IRSNB: Institut royal des Sciences naturelles de Belgique, Bruxelles, Belgium; MNHN: Muséum national d'Histoire naturelle, Paris, France; RH: R. Houart Collection; USNM: National Museum of Natural History, Washington, DC, USA; ad: adult; dd: collected empty; juv: juvenile; lv: collected alive.

Terminology used to describe the spiral cords and the apertural denticles (after Merle 2001, 2005) (Figures 7, 8, 24, 27, 40, 41). Terminology in parentheses: variable feature.

Convex part of teleoconch whorl and siphonal canal: Adis: Adapical infrasutural secondary cord on subsutural ramp; IP: Infrasutural primary cord on subsutural ramp; P1–P6: Primary spiral cords on the convex part of the teleoconch whorl and the siphonal canal; s1–s5: Secondary cord of the convex part of the teleoconch whorl (for example, s1: Secondary cord of the convex part of the teleoconch whorl between P1 and P2); ADP: Adapertural primary cord on the siphonal canal; MP: Median primary cord on the siphonal canal; ABP: Abapertural primary cord on the siphonal canal.

Aperture: ID: infrasutural denticle; D1 to D6: abapical denticles.

SYSTEMATICS

Family Muricidae Rafinesque, 1815
Subfamily Muricopsinae Radwin and D'Attilio, 1971

Genus *Favartia* Jousseaume, 1880

Type Species: *Murex breviculus* Sowerby II, 1834, Indo-West Pacific, by original designation.

Favartia aquinoi new species

Figures 6, 7–19

Type Material: Holotype IRSNB MT.3801/I.G.34044, 1 paratype coll. Wanderley Vieira de Aquino Junior, Sao Paulo, Brazil; 1 paratype R. Houart, all from the type locality.

Type Locality: Brazil, Rio de Janeiro State, off Arraial do Cabo, 30–35 m, 2008.

Other Material Examined: Brazil, Ilha do Pai, 16 m, 1960, RH (1 dd, ad); Ilha de São Sebastião, 35–45 m, in sand, 1992, RH (2 lv, ad); Vitoria Bank, 52 m, 1987, RH (1 dd, juv).

Distribution: Brazil, from Vitória Bank to Ilha de São Sebastião, living at 35–45 m.

Description: Shell medium sized for the genus, up to 17.9 mm in length. Height/width ratio 1.9–2.0. Slender, lanceolate, biconical, broadly ovate. Very weakly spinose, nodose, lightly built. Subsutural ramp moderately broad, weakly sloping, weakly concave. Shell color creamy white or light tan with occasional brown spots on subsutural ramp, between axial varices. Aperture pale white within.

Spire high, with 1.5 protoconch whorls and up to 5 broad, convex, strongly shouldered teleoconch whorls. Suture impressed. Protoconch large, broad. Whorls rounded. Maximum width and height 900 µm. Axial sculpture of teleoconch whorls consisting of low, narrow, weakly frondose varices. Each varix with very short, frondose, open, primary spines. First teleoconch whorl with 8 varices, second with 8 or 9, third to penultimate whorl with 9, last whorl with 7 or 8 varices. Spiral sculpture of high, rounded, narrow, weakly nodose primary and secondary cords consisting of (adis), IP, P1–ABP. Adis and IP shallow, giving rise to a small, curved, short spine at intersection of axial varices. P1–P5 of same height and wide on last teleoconch whorl; P6 quite narrower and lower, followed by ADP, MP, and ABP, ADP, and MP of same strength as P1–P5; ABP somewhat smaller. Low, blunt, open spines originate at crossing of axial varices and spiral cords, more apparent on apertural varix. Aperture moderately large, ovate. Columellar lip narrow, smooth. Rim partially erect, adherent at small portion at adapical extremity. Anal notch shallow, broad. Outer lip erect, crenulated, with low ID and D1–D6 within. Siphonal canal short, 18–21% of total shell length, narrow, weakly dorsally recurved, narrowly open, with short, blunt spines corresponding to ADP, MP, and ABP, decreasing in length abapically. Operculum and radula unknown.

Remarks: *Favartia aquinoi* new species may be compared with *F. glypta* (= *Murexiella iemanja*) which also occurs in Brazil, with *F. cellulosa*, living from Florida to Brazil, and with *F. levicula* known from North Carolina to the Gulf of Mexico. The most similar species, *F. glypta* (Figures 2–5, 20–23, 24–31), differs from *F. aquinoi* new species in having a somewhat smaller shell in Recent specimens with a smaller protoconch, a lower spire, narrower and more squamous primary spiral cords, more distant from each other, a very narrow s2 cord and a narrower siphonal canal with short ADP, MP, and occasionally ABP, spines. These differences can already be observed in juvenile specimens of both species, for example in the holotype of *Murexiella iemanja* (8 mm) (Figures 20–21) and a young *F. aquinoi* new species (5.4 mm) (Figures 17–19). *Favartia cellulosa* (Figures 32–34), mostly known from Florida, but

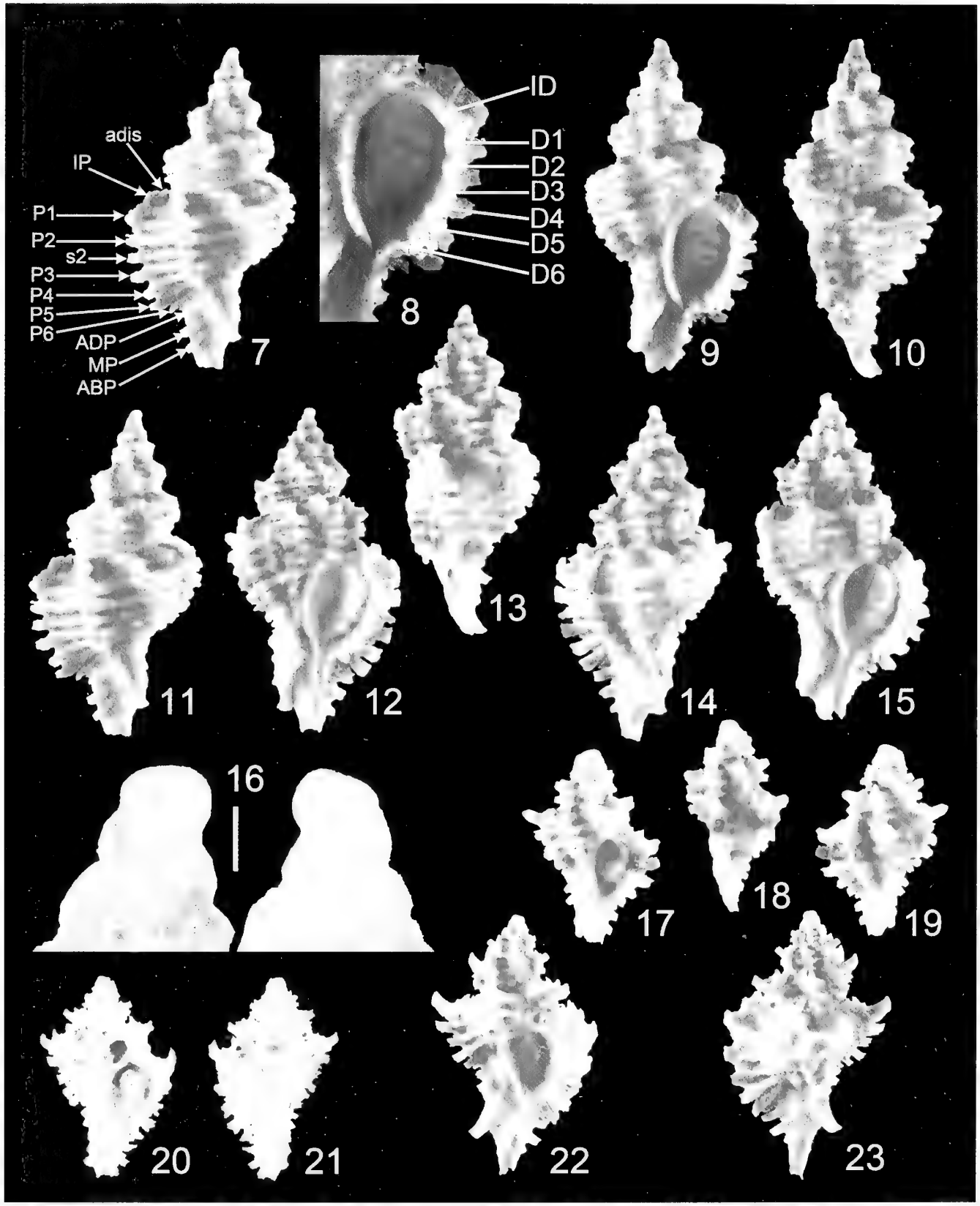

Figures 7–23. *Favartia species*. **7–19. *Favartia aquinoi* new species** Brazil, Rio de Janeiro State, off Arraial do Cabo, 30–35 m, sand and rubble, Sept. 2008. **7–11.** Holotype MT.3801/I.G.34044, 17.8 mm. **12–14.** Paratype RH, 17.9 mm.**15.** Paratype coll. Wanderley Vieira de Aquino Junior, 16.4 mm. **16.** Protoconch (paratype RH), crushed afterwards. **17–19.** Brazil, Vitória Bank, 20°32' S, 38°11' W, 52 m, RH, 5.3 mm. **20–23.** *Favartia glypta* (M. Smith, 1938). **20–21.** Brazil, Bahia State, 2 km E Santa Bárbara Id., Abrolhos Archipelago, Chapeirão reef, 25 m, holotype of *Murexiella iemanja* Petuch, 1979, USNM 780652, 7.8 mm (photo courtesy USNM). **22–23.** Brazil, Espírito Santo State, off Guarapari, 45–60 m, June 2012, RH, 10.6 mm. Scale bars (also for Figure 25) = 500 μm.

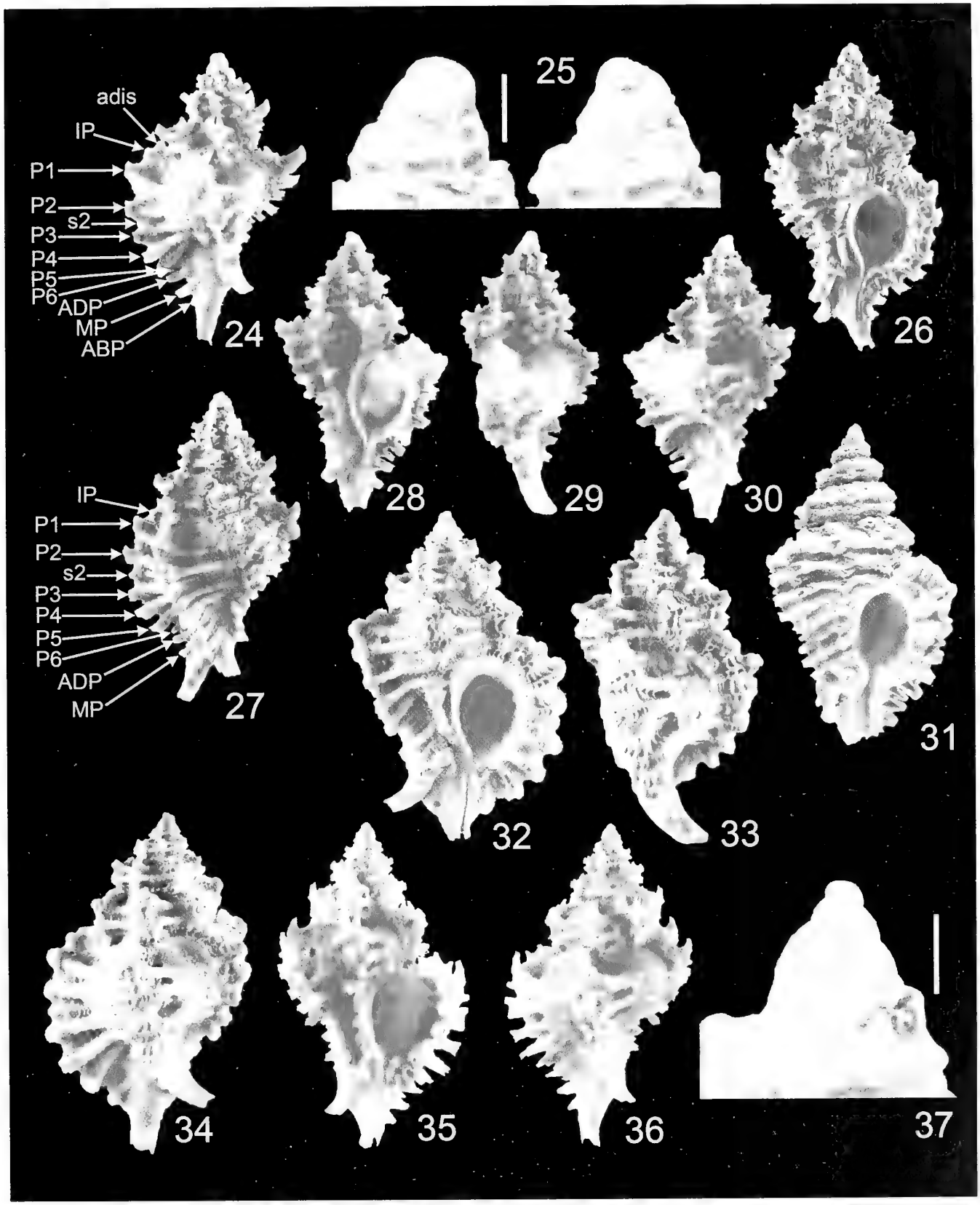

Figures 24–37. *Favartia species*. **24–31.** *Favartia glypta* (M. Smith, 1938). **24–25.** Brazil, Espírito Santo State, off Guarapari, 45–60 m, June 2012, RH, 10.6 mm. **26–27.** Colombia, southern Cartagena, off Golfo de Morrasquillo, 100 m, March 2005, RH, 13.9 mm. **28–30.** Brazil, Espirito Santo State, off Guarapari, 25m, Nov. 1993, RH, 11.1 mm. **31.** Brazil, Espirito Santo State, Gurapari Channel, muddy area, low tide, April 1995, RH, 15.4 mm. **32–34.** *Favartia cellulosa* (Conrad, 1846). Florida, West of Boca Raton, 54 m, rubble bottom, RH, 16.2 mm. **35–37.** *Favartia levicula* (Dall, 1889). **35–36.** Florida (no other data), RH, 15.5 mm. **37.** Florida, Southwest of Panama City, dredged 55 m, protoconch, RH. Scale bar = 500 μm.

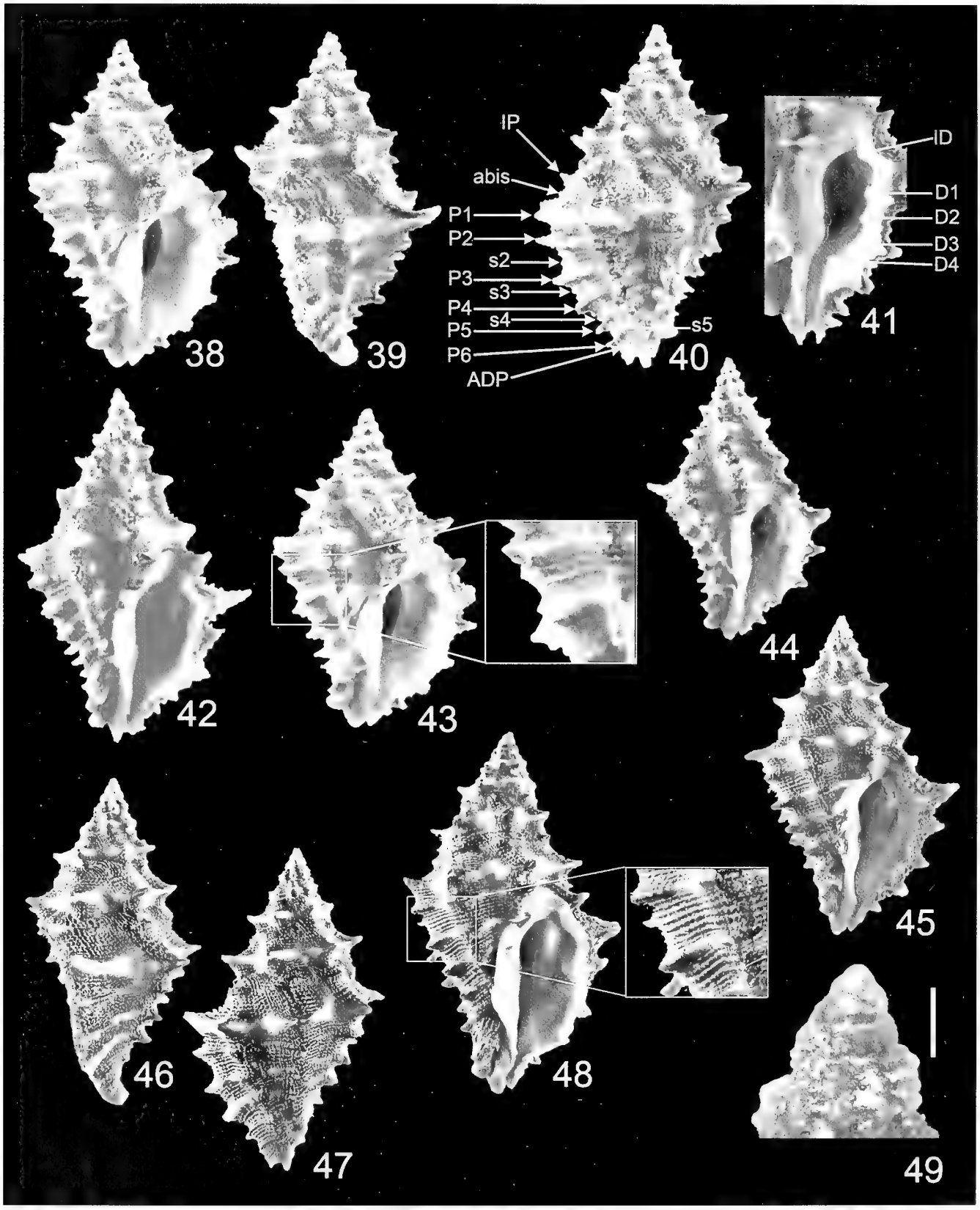

Figures 38–49. *Muricopsis* species. **38–44.** ***Muricopsis (Muricopsis) vassarti* new species. 38–41, 43.** Pacific Panama, Archipiélago de las Perlas, 1997, holotype MNHN-IM-2000-305226, 22.8 mm. **42.** Pacific Panama, Archipiélago de las Perlas, Isla Pedro Gonzales, 8° N, 79° W, 2002, paratype RH, 23.4 mm. **44.** Pacific Panama, Archipiélago de las Perlas, Isla Pedro Gonzales, 8° N, 79° W, 2002, paratype RH, 18.9 mm. **45–49.** *Muricopsis (Muricopsis) zeteki* Hertlein and Strong, 1951. **45–47.** Pacific Panama, Archipiélago de las Perlas, 1997, RH, 21.0 mm. **48.** Pacific Panama, Archipiélago de las Perlas, Isla Pedro Gonzales, 8° N, 79° W, 2002, RH, 28.3 mm. **49.** Protoconch, Pacific Panama, Archipiélago de las Perlas, Isla Pedro Gonzales, 8° N, 79° W, 2002, RH. Scale bar = 500 μm.

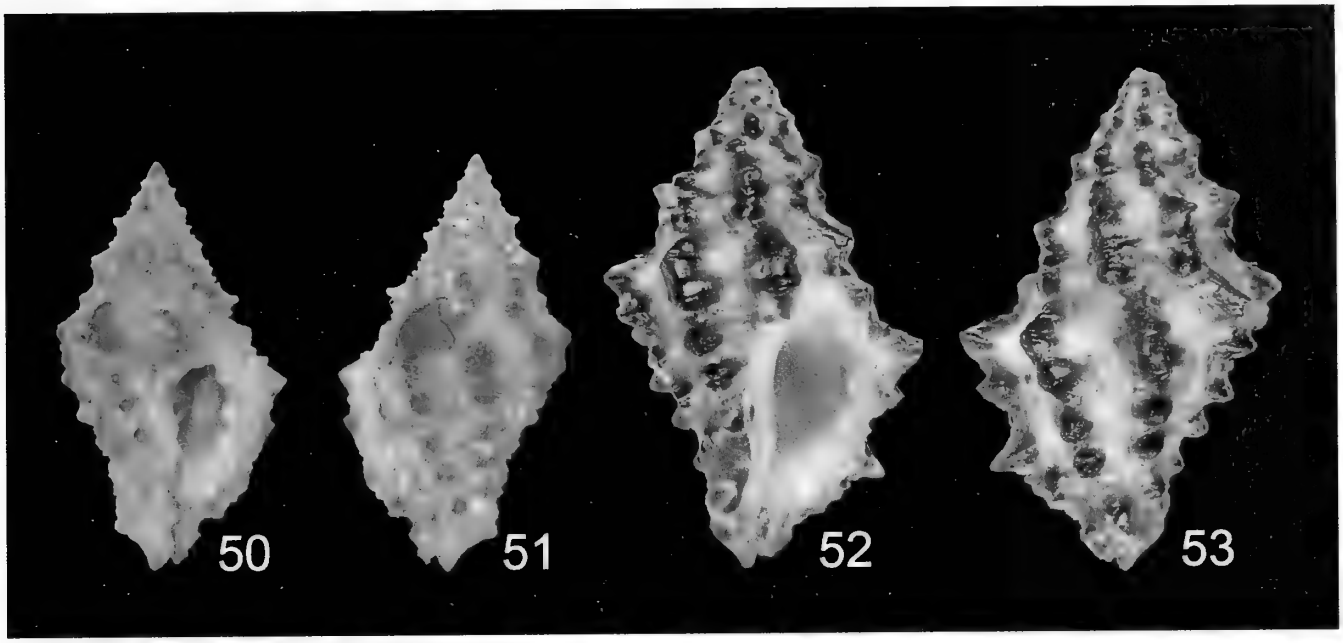

Figures 50–53. *Muricopsis* species. **50–51.** *Muricopsis (Muricopsis) westonensis* Myers and D'Attilio, 1990, Costa Rica, Cocos Id, Bahia Weston, 12 m, under dead coral, April 1983, holotype USNM 860014, 13.4 mm (photo courtesy USNM). **52–53.** *Muricopsis (Muricopsis) taupini* Garrigues, 2016. Galapagos, off Santiago Ids, Albany Id, 5–15 m, on rocks, holotype MNHN-IM-2000-31680, 19.9 mm (photo Manuel Caballer, MNHN).

extending its geographical distribution to Brazil, differs in having a broader shell, a smaller protoconch, comparatively narrower primary cords, almost obsolete P6 cord and spine, shorter or almost obsolete, broad, blunt P1–P6 spines, broader and fewer axial varices, and a broader siphonal canal, strongly tapered abapically, with a short ADP spine. *Favartia levicula* (Figures 35–37) differs in having a broader shell with a lower spire, broader and flatter primary spiral cords, obsolete or strongly reduced between each pair of axial varices, a shorter siphonal canal, strongly adapically tapered, and chiefly in having a conical protoconch of 3.5 whorls, denoting planktotrophic larval development (Figure 37), as opposed to a broad, globose, paucispiral protoconch in *F. aquinoi* new species (Figure 16). *Favartia glypta* was considered a junior synonym of *F. levicula* by Radwin and D'Attilio (1976: 159), but this was certainly due to Clench and Pérez-Farfante (1945: 56, pl. 28, figs 1–3), who illustrated two specimens of *F. glypta* as *Murex cellulosus leviculus*, following in that the taxonomy of M. Smith (1939: 16, pl. 13, fig. 8).

Etymology: I am pleased to follow the request of Marcus Coltro, naming this new species after Wanderley Vieira de Aquino Junior, shell collector from São Paulo and past president of *Conquiliologistas do Brasil*.

Genus *Muricopsis* Bucquoy and Dautzenberg, 1882

Subgenus *Muricopsis* Bucquoy and Dautzenberg, 1882

Type Species: *Murex blainvillei* Payraudeau, 1826 (= *Murex cristatus* Brocchi, 1814), Mediterranean, by original designation.

Muricopsis (*Muricopsis*) *vassarti* new species

Figures 6, 38–44

Type Material: Holotype, MNHN-IM-2000-305226, Pacific Panama, Archipiélago de las Perlas, 1997; 3 paratypes, Pacific Panama, Archipiélago de las Perlas, Isla Pedro Gonzales, 8° N, 79° W, 2002, R. Houart.

Type Locality: Pacific Panama, Archipiélago de las Perlas.

Distribution: Pacific Panama, Archipiélago de las Perlas.

Description: Shell medium-sized for the genus, up to 23.4 mm in length. Height/width ratio 1.6. Lanceolate, biconical, broad. Heavy and spinose. Subsutural ramp broad, strongly sloping, strongly concave. Light brown with darker brown spots on axial varices, between and on spines. Creamy white on dorsal side of spines. Aperture glossy white. Spire high, acute. Protoconch whorls eroded. Teleoconch of up to 8 angulate, strongly shouldered, spinose whorls. Suture weakly adpressed.

Axial sculpture of teleoconch whorls consisting of narrow, high ribs on first teleoconch whorls and high, broad, sharp spinose varices from fourth to last whorl. First to penultimate whorl with 7 or 8 ribs or varices. Last whorl with 6 varices. Spiral sculpture of low, strong, narrow, squamous primary and secondary cords and few threads. Last teleoconch whorl with broad IP, occasional abis, followed by P1, P2, s2, P3, s3, P4, s4, P5, (s5), P6, ADP. Primary cords giving rise to short, acute, triangular, open spines on axial varices. Aperture large, ovate. Columellar lip moderately broad, weakly flaring, with 2 elongate, strong folds abapically. Rim partially

erect, adherent at a small portion at adapical extremity. Very low parietal tooth at adapical extremity. Anal notch deep, narrow. Outer lip weakly erect, crenulated, with 5 strong denticles within, decreasing in strength abapically, consisting of IP, D1–D4. Siphonal canal short, 11–15% of total shell length, broad, weakly dorsally recurved, open, with acute, short P6 and ADP spines. Operculum dark brown, strongly ovate with apical nucleus in lower right. Radula unknown.

Remarks: The four studied specimens of *Muricopsis vassarti* new species were collected living in syntopy with two lots of *M. zeteki*, the latter being obviously more numerous. One specimen, the holotype of *M. vassarti* new species and 12 specimens of *M. zeteki* were taken in one spot, three specimens (paratypes RH) were collected in the other spot, together with 9 specimens of *M. zeteki*. Both lots were left unseparated during many years, until a recent short review of the *Muricopsis* and *Murexsul* species in my collection. *Muricopsis zeteki* (Figures 45–49) differs from the new species in having a blackish brown and white coloured shell and a different spiral sculpture. In *M. zeteki* there are 4–6 narrow spiral threads between each pair of primary cords (Figures 48) as opposed to a single small secondary cord and one or two additional threads in *M. vassarti* new species (Figure 43). In *M. zeteki* the primary cords are also narrower. The protoconch of *M. vassarti* new species was eroded in all examined specimens but could be paucispiral, consisting of 1.25 whorls (see below). It is conical and multispiral, consisting of 3 whorls in *M. zeteki* (Figure 49) denoting planktotrophic larval development, which may explain its extended geographical distribution from the northern Gulf of California to North Peru and the Galapagos Islands. Garrigues (2016: 8) in his description of *M. taupini* described the protoconch of *M. zeteki* as being paucispiral, consisting of 1.25 whorls. The illustrated protoconch (Garrigues, 2016, figs 3I–J) is from a juvenile specimen collected at Boyerana Id, in the Archipiélago de las Perlas and shows indeed a paucispiral protoconch. However, the shell (fig. 3I) looks much closer to *M. vassarti* new species and could be a juvenile specimen of that species. *Muricopsis westonensis* from the Pacific coast of Costa Rica (Figures 50–51) differs from *Muricopsis vassarti* new species in having a smaller, narrower shell with a somewhat less acute spire, a narrower aperture and stronger folds on the columellar lip. It is also less spiny with low, brown coloured knobs at intersection of spiral and axial sculpture instead of sharp, whitish spines in *M. vassarti* new species. Finally, *Muricopsis taupini* from the Galapagos (Figures 52–53) is different in having a smaller shell with a lower spire, lower columellar folds and apertural denticles, a shorter siphonal canal and blunt, blackish brown knobs.

Etymology: Named for André Vassart who collected these specimens in 1997 and 2002, traveling aboard his vessel La Boudeuse.

ACKNOWLEDGMENTS

I am very grateful to Jose and Marcus Coltro, Brazil, who sent me the *Favartia* specimens for study a few years ago, to Ellen Strong, National Museum of Natural History, Washington, DC, USA, for the permission she gave to use the images from USNM, to Manuel Caballer (MNHN) who provided the images of the MNHN holotype of *Muricopsis taupini* (E-Recolnat Project: ANR-11-INBS-0004), to Emily H. Vokes, Ponchatoula, Louisiana, USA, for permission to reproduce her photo of the holotype of *Favartia glypta*, and as always, to John Wolff, Lancaster, Philadelphia, USA, for checking the English text and for other comments. Many thanks also to the reviewers, Yuri Kantor and Jerry Harasewych for their useful advice.

LITERATURE CITED

Bouchet, P. and Yu.I. Kantor. 2004. New Caledonia: the major center of biodiversity for volutomitrid mollusks (Mollusca: Neogastropoda: Volutomitridae). Systematics and Biodiversity, 1(4): 467–502.

Clench, W.J. and I. Pérez-Farfante 1945. The genus *Murex* in the Western Atlantic. Johnsonia 1(17): 1–56.

Fair, R.H. 1976. The Murex Book, an illustrated catalogue of Recent Muricidae (Muricinae, Muricopsinae, Ocenebrinae), Sturgis Printing Co., Honolulu, Hawaii: 138 pp.

Garrigues, B. 2016. Description d'une nouvelle espèce de *Muricopsis* (Gastropoda: Muricidae: Muricopsinae) des Iles Galapagos. Xenophora Taxonomy 11: 3–8.

Houart, R. 1991. The Southeastern Brazilian Muricidae collected by R.V. Marion-Dufresne in 1987, with the description of three new species. The Nautilus 105: 26–37.

Houart, R. 2018. Historique et classification des espèces actuelles de Muricidae (Neogastropoda, Muricoidea). Novapex 19(2): 37–66.

Kaicher, S.D. 1974. Card catalogue of world-wide shells, Muricidae II, Pack 6. Privately publ. St. Petersburg, Florida.

Kaicher, S.D. 1978. Card catalogue of world-wide shells, Muricidae III, Pack 16. Privately publ. St. Petersburg, Florida.

Kaicher, S.D. 1980. Card catalogue of world-wide shells, Muricidae V. Pack 25. Privately publ. St. Petersburg, Florida.

Kaicher, S.D. 1991. Card catalogue of world-wide shells, Muricidae VI. Pack 59. Privately publ. St. Petersburg, Florida.

Keen, A.M. 1971. Sea shells of Tropical West America, Marine Mollusks from Baja California to Peru. 2d edit. Stanford University Press, Stanford, California: i–xiv, 1–1064.

Merle, D. 2001. The spiral cords and the internal denticles of the outer lip in the Muricidae: terminology and methodological comments. Novapex 2(3): 69–91.

Merle, D. 2005. The spiral cords of the Muricidae (Gastropoda, Neogastropoda): importance of ontogenetic and topological correspondences for delineating structural homologies. Lethaia 38: 367–379.

Merle, D. and R. Houart. 2003. Ontogenetic changes of the spiral cords as keys innovation of the muricid sculptural patterns: the example of the *Muricopsis-Murexsul* lineages (Gastropoda: Muricidae: Muricopsinae). Comptes Rendus Palevol 2: 547–561.

MolluscaBase. 2019a. *Favartia*. http://www.marinespecies.org/aphia.php?p=taxdetails&id=206015. Accessed through: World Register of Marine Species on 2019-06-30.

MolluscaBase. 2019b. *Muricopsis*. http://www.marinespecies.org/aphia.php?p=taxdetails&id=138198. Accessed through: World Register of Marine Species on 2019-06-30.

Myers, B.W. and A. D'Attilio. 1990. Three new Muricacean species from Cocos Island, Costa Rica (Muricidae and Coralliophilidae). Venus 49(4): 281–292.

Radwin G. and A. D'Attilio. 1976. *Murex* shells of the world. An illustrated guide to the Muricidae. Stanford University Press, Stanford, 284 pp.

Rios, E.C. 1985. Seashells of Brazil. Rio Grande, RS, 328 pp.

Smith, M. 1939. An illustrated catalog of the Recent species of the Rock Shells. Muricidae, Thaisidae and Coralliophilidae. Tropical Laboratory, Lantana, Florida, v–ix + 84 pp.

Vokes, E.H. 1971. Catalogue of the genus *Murex* Linné (Mollusca: Gastropoda. Muricinae, Ocenebrinae. Bulletin of American Paleontology 61(268): 1–141.

Vokes, E.H. 1994. Cenozoic Muricidae of the western Atlantic region. Part X – The subfamily Muricopsinae. Tulane Studies in Geology and Paleontology 26(2–4): 49–160.

Description of two new species (Bivalvia: Vesicomyidae, Verticordiidae) from a cold seep in the South China Sea

Jinxiang Jiang
Third Institute of Oceanography
Ministry of Natural Resources
Xiamen, 361005, CHINA

Yaqin Huang
Third Institute of Oceanography
Ministry of Natural Resources
Xiamen, 361005, CHINA
and
Fisheries College
Jimei University
Xiamen, 361021, CHINA

Qianyong Liang
MLR Key Laboratory of Marine Mineral Resources
Guangzhou Marine Geological Survey
China Geological Survey
Guangzhou, 510070, CHINA

Junlong Zhang[1]
Institute of Oceanology
Chinese Academy of Sciences
Qingdao, 266071, CHINA
and
Center for Ocean Mega-Science
Chinese Academy of Sciences
Qingdao, 266071, CHINA

ABSTRACT

In this paper, we describe two new deep-sea bivalve species belonging to the families Vesicomyidae and Verticordiidae, respectively. They were collected during a survey of the Haima Methane Seep at the Qiongdongnan Basin on the northwestern slope of the South China Sea, China, at a depth of 1,400 m. *Vesicomya rhombica* new species is small in size and characterized by its rhombic shell shape and a slight furrow on the surface of the posterior shell region, running from the umbo to the postero-ventral margin. It is the first species of this genus recorded from Chinese waters. *Spinosipella xui* new species has a long, lamellar posterior lateral tooth on the right valve, 13 strong radial ribs, and conspicuous spines on the shell surface. The latter constitutes one of three species of this genus living in Chinese waters.

Additional Keywords: new species, *Vesicomya*, *Spinosipella*, Vesicomyidae, Verticordiidae, taxonomy, chemosymbiotic environment

INTRODUCTION

Many habitats remain underexplored in the bathyal and abyssal seafloor that draw significant concerns worldwide. Our knowledge of the biodiversity of deep-sea mollusks remains quite limited due to technological difficulties in the access to this perpetually dark world and resulting insufficient sampling, which results in controversial explanations of their fauna, biodiversity, and biogeography (Arbizu and Brix, 2008; Brökeland and George, 2009). With the gradual increase in exploration of the deep-sea, vast numbers of mollusks have been sampled. Reporting newly found species is imperative to understanding the biodiversity of the deep-sea, as accurate identifications and taxonomy are crucial and the foundation for further studies.

[1] Corresponding author: zhangjl@qdio.ac.cn

The Vesicomyidae Dall and Simpson, 1901 is a deep-sea bivalve family, distributed worldwide from about 100 m to more than 10,000 m depth in the abyssal and hadal zones (Krylova et al., 2018). It has received mounting attention due to its specialized habitat. Most of the members are confined to chemosynthetic communities such as cold seeps, hydrothermal vents, whale carcasses, or other sulphide-rich reducing environments (Krylova and Sahling, 2010; Coan and Valentich-Scott, 2012; Krylova et al., 2018). This family is considered to include two subfamilies, Vesicomyinae Dall and Simpson, 1901 and Pliocardiinae Woodring, 1925, totaling more than 125 Recent species (Krylova and Sahling, 2010; Decker et al., 2012; Johnson et al., 2017; Krylova et al., 2018). These two subfamilies are well-supported and widely accepted (Krylova and Sahling, 2010; Valdés et al., 2012). *Vesicomya* Dall, 1886 is the only genus of Vesicomyinae; included species are generally small in size and mainly inhabit abyssal plains or hadal trenches. Krylova and Sahling (2010) assigned 18 species to this genus. But as it was not delimited well, *Vesicomya* had long been employed as a catchall taxon, to which many vesicomyids from hydrothermal vent and cold seep ecosystems were originally or subsequently assigned, sometimes rather incongruently (Coan et al., 2000).

The name *Vesicomya* is often used between quotation marks when the taxonomic status of a vesicomyine species is not well resolved, e.g., as in *"Vesicomya" filatovae* Krylova and Kamenev, 2015 (Krylova et al. 2015). Conversely, some of its included species were assigned even to different families or genera such as *Kelliella* or *Callocardia*. Krylova et al. (2018) re-clarified the relationship between *Vesicomya* and *Kelliella*, and assigned 15 species to *Vesicomya*.

The family Verticordiidae Stoliczka, 1870 is another common group of deep-water bivalves. Most members are mobile infaunal carnivores that exclusively inhabit the deep-sea (Coan and Valentich-Scott, 2012). At least 11 genera and more than 90 species have been reported for

this family (Huber, 2010). *Spinosipella* Iredale, 1930 is one of species-poor genus of verticordiids. Simone and Cunha (2008) comprehensively revised this genus by studying both conchological and anatomical characters. Nowadays, five valid species are assigned to the genus: *S. acuticostata* (Philippi, 1844), *S. agnes* Simone and Cunha, 2008, *S. tinga* Simone and Cunha, 2008, *S. deshayesiana* (P. Fischer, 1862) (= *Verticordia japonica* A. Adams, 1862= *Verticordia ericia* Hedley, 1911), and *S. costeminens* (Poutiers, 1981).

Vesicomyids are well represented in the northern Pacific (Krylova and Janssen, 2006), but the biodiversity in Chinese waters is poorly known. Up to now, only two large species of this family were described from the South China Sea, *Laubiericoncha nanshaensis* (Xu and Shen, 1991) and *Archivesica marissinica* (Chen, Okutani, Liang and Qiu, 2018). However, no *Vesicomya* species were found. Regarding Verticordiidae, a total of 6 species have been reported from Chinese waters (Liu, 2008). Among them, two species belong to genus *Spinosipella* i.e., *S. deshayesiana* and *S. costeminens* (Liu, 2008; Xu and Zhang, 2008).

During the recent survey HYIV20150402 to the Qiongdongnan Basin on the northwestern slope of the South China Sea by R/V Hai Yang Si Hao, a new vesicomyid belonging to *Vesicomya* and a new verticordiid belonging to *Spinosipella* were collected. Herein, we described them as new.

MATERIALS AND METHODS

Specimens studied were collected by bottom trawling with RV Hai Yang Si Hao from recently discovered Haima Methane Seep about 1,400 m depth off southern Hainan Island in the northern sector of the South China Sea, April 2nd, 2015 (Liang et al., 2017; Feng et al., 2018). Together with the specimens, this trawling also sampled 134 individuals of *Bathymodiolus platifrons* Hashimoto and Okutani, 1994, and 9 of *Archivesica marissinica* (Chen, Okutani, Liang and Qiu, 2018), which are typical vent and seep specialized chemosymbiotic bivalves. Figure 1 shows a map of the collecting site.

Shells were observed using a Zeiss Discovery V12 stereo microscope. Photographs were taken using a Cannon EOS6D camera or a Zeiss AxioCam 503 digital camera coupled to the microscope. Measurements were made with a Vernier caliper to the nearest 0.1 mm. All specimens were collected dead and dried by Dr. Xuebao He, so hindering examination of soft parts. Type specimens are deposited in the Third Institute of Oceanography, Ministry of Natural Resources, Xiamen, China. The terminology for morphological description and hinge teeth of Vesicomyidae was used following Cox (1969), von Cosel and Salas (2001), Krylova and Janssen (2006), Amano and Kiel (2007). Abbreviations: SL, shell length; SH, shell height; SW, shell width.

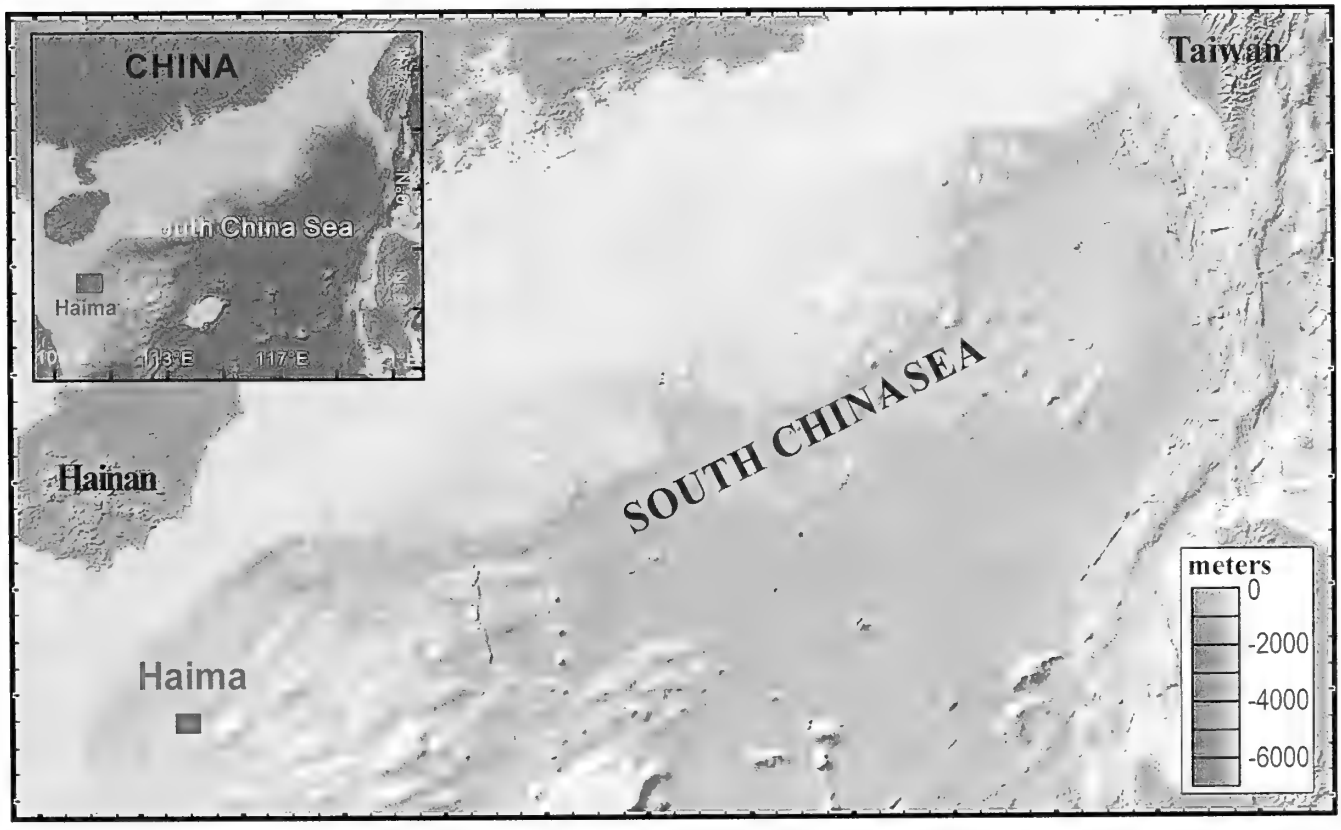

Figure 1. Map of the South China Sea showing the location of Haima Methane Seep, indicated by a rectangle (modified from Liang et al., 2017).

SYSTEMATICS

Superfamily Glossoidea Gray, 1847 (1840)
Family Vesicomyidae Dall and Simpson, 1901
Subfamily Vesicomyinae Dall and Simpson, 1901

Genus *Vesicomya* Dall, 1886
Callocardia (Vesicomya) Dall, 1886: 272.

Type Species: *Callocardia atlantica* Smith, 1885 (by original designation).

***Vesicomya rhombica* new species**
(Figures 2–7)

Description: Shell small, 7.10–8.20 mm long, fragile, thin, rhombic in shape, inequilateral, equivalve. Anterior dorsal margin depressed, concave; anterior end evenly rounded; posterior dorsal margin sloping, slightly convex; posterior end faintly angulate; ventral margin long and rather convex. Umbones protruding, ascending; beaks prominent, strongly prosogyrate, situated at the middle of dorsal margin. Surface white, porcellaneous, sculpture of commarginal striae and low regular ribs. Periostracum thin, glossy, translucent. Slight furrow running from umbo to postero-ventral margin present on posterior area of shell. Lunule triangular, sunken, distinct, demarcated by incision. Escutcheon indistinct. Ligament external, opisthodetic, strong, 1/3 length of posterior dorsal margin, attached to nymphs on outer edge of posterior hinge plate. Internal surface of valves white, smooth. Hinge plate narrow. On right valve, anterior cardinal tooth 1 wedge-like, located on ventral margin of hinge plate, its elongated high posterior end located under anterior ramus 3a of posterior cardinal tooth, posterior ramus 3b thicker, radiated posteriorly. On left valve, anterior cardinal tooth long, bifid, V-shaped, with anterior 2a tooth long, along ventral margin of hinge plate, fused with anterior edge of middle 2b tooth; posterior cardinal tooth 4b elongated, parallel to postero-dorsal margin of the shell. Adductor muscle scars distinct, anterior teardrop-shaped, anterior pedal retractor scar small, impressed, located dorsally to and fused with anterior adductor scar; posterior adductor scar reniform, larger than the anterior one; Pallial line without pallial sinus.

Type Material: Holotype: TIO-BTS-MOL-1601 (Sta.QDN31), 1 specimen, SL 8.20 mm, SH 6.60 mm, SW 4.40 mm. Paratype: TIO-BTS- MOL-1602(Sta.QDN31), 1 specimen, SL 7.10 mm, SH 5.60 mm, SW 3.80 mm. All from type locality.

Type Locality: Haima Methane Seep, muddy bottom, about 1,400 m depth off southern Hainan Island in the northern sector of the South China Sea.

Distribution: Known only from type locality.

Etymology: The Latin specific epithet *rhombica* refers to the rhombic shell shape in this species.

Remarks: The new species can be distinguished from other congeners by its rhombic shell shape and a slight furrow at the surface posterior area running from the umbo to the postero-ventral margin. Among the 15 species within this genus assigned by Krylova et al. (2018), seven of them are distributed in the Indo-West Pacific: *Vesicomya galatheae* (Knudsen, 1970), *V. pacifica* (E.A. Smith, 1885), *V. tasmanensis* (Knudsen, 1970), *V. bruuni* Filatova, 1969, *V. sundaensis* (Knudsen, 1970), *V. profundi* Filatova, 1971, and *V. sergeevi* Filatova, 1971 (Krylova et al., 2015). In addition to differences in shell shape, the first five species differ from the new species by the arrangement of the ventral anterior cardinal tooth 1 and anterior ramus 3a on the right valve, which do not overlap. Instead, in the new species, the elongated high posterior end of the cardinal tooth 1 is located under anterior ramus 3a of the posterior cardinal tooth on the right valve. The hinge of the new species is very similar to those of *V. profundi* and *V. sergeevi*, both of which are found in the Kuril-Kamchatka Trench, northwest Pacific (Krylova et al., 2015; Kamenev, 2019). But they differ by their shell shape and sculpture. The shell of *V. profundi* is subcircular in outline, higher, more inflated, and shorter in its anterior and posterior ends, with the umbo protruding. Both the new species and *V. sergeevi* have less inflated and longer shells. But *V. sergeevi* is ovoid in shape, has less conspicuous commarginal ribs, and lacks the furrow on the posterior area. *Vesicomya indica* (Knudsen, 1970), first found in the central Indian Ocean, was also reported from southern Shikoku, Japan (Tsuchida, 1994; Higo, Callomon and Goto, 1999). But from the published figures (Tsuchida 1994: 78, fig. 3, pl. 3, figs. 1, 2), we can ascertain that it is definitely not *V. indica*. Another species from Japan, *V. katsuae* Kuroda, 1952 was assigned to *Waisiuconcha* by Higo, Callomon, and Goto (1999: 2001). Krylova and Janssen (2006) observed that it should be excluded from the genus *Waisiuconcha*. Huber (2010) allocated the species in the genus *Isorropodon*. Okutani (2017) still included the species in *Vesicomya*, as originally determined by Kuroda (1952). However, from the type figure (Kuroda, 1952: 4, text-figs. 5–9; Higo, Callomon and Goto, 2001: 174, fig. B1099), we believe that it may belong to the genus *Pliocardia*, pending further confirmation.

Superfamily Verticordioidea Stoliczka, 1870
Family Verticordiidae Stoliczka, 1870

Genus *Spinosipella* Iredale, 1930
Spinosipella Iredale, 1930: 388

Type Species: *Verticordia ericia* Hedley, 1911 (original designation).

***Spinosipella xui* new species**
(Figure 8–13)

Description: Shell small, 4.7 mm in length, inflated, quadrangular or square-rhombus shaped, inequilateral, weakly coiled, inequivalve, right valve slightly larger and

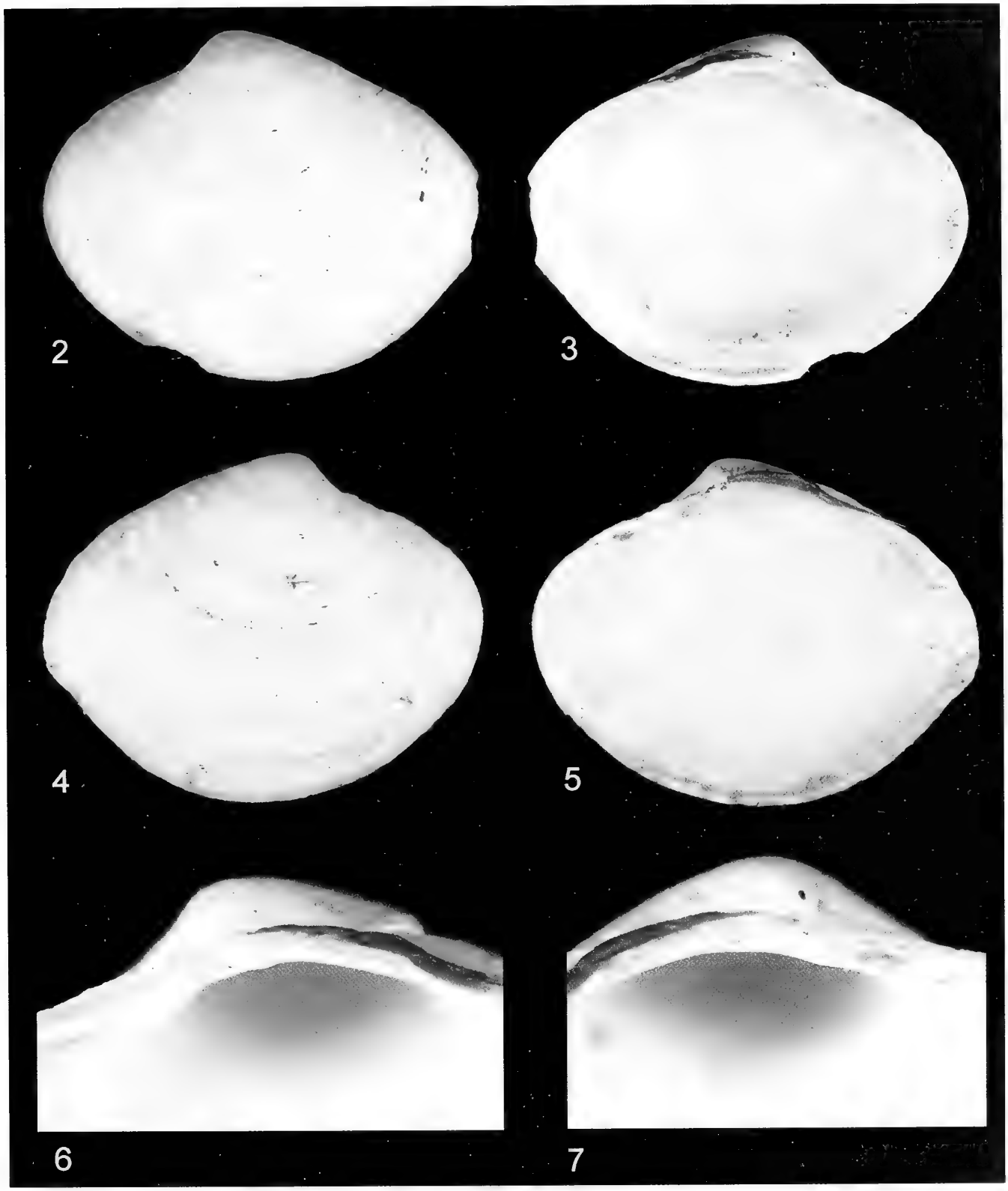

Figures 2–7. ***Vesicomya rhombica*** **new species,** holotype (TIO-BTS-MOL-1601). **2.** Exterior of left valve. **3.** Interior of left valve. **4.** Exterior of right valve. **5.** Interior of right valve. **6–7.** Details of hinges. **6.** Right valve. **7.** Left valve.

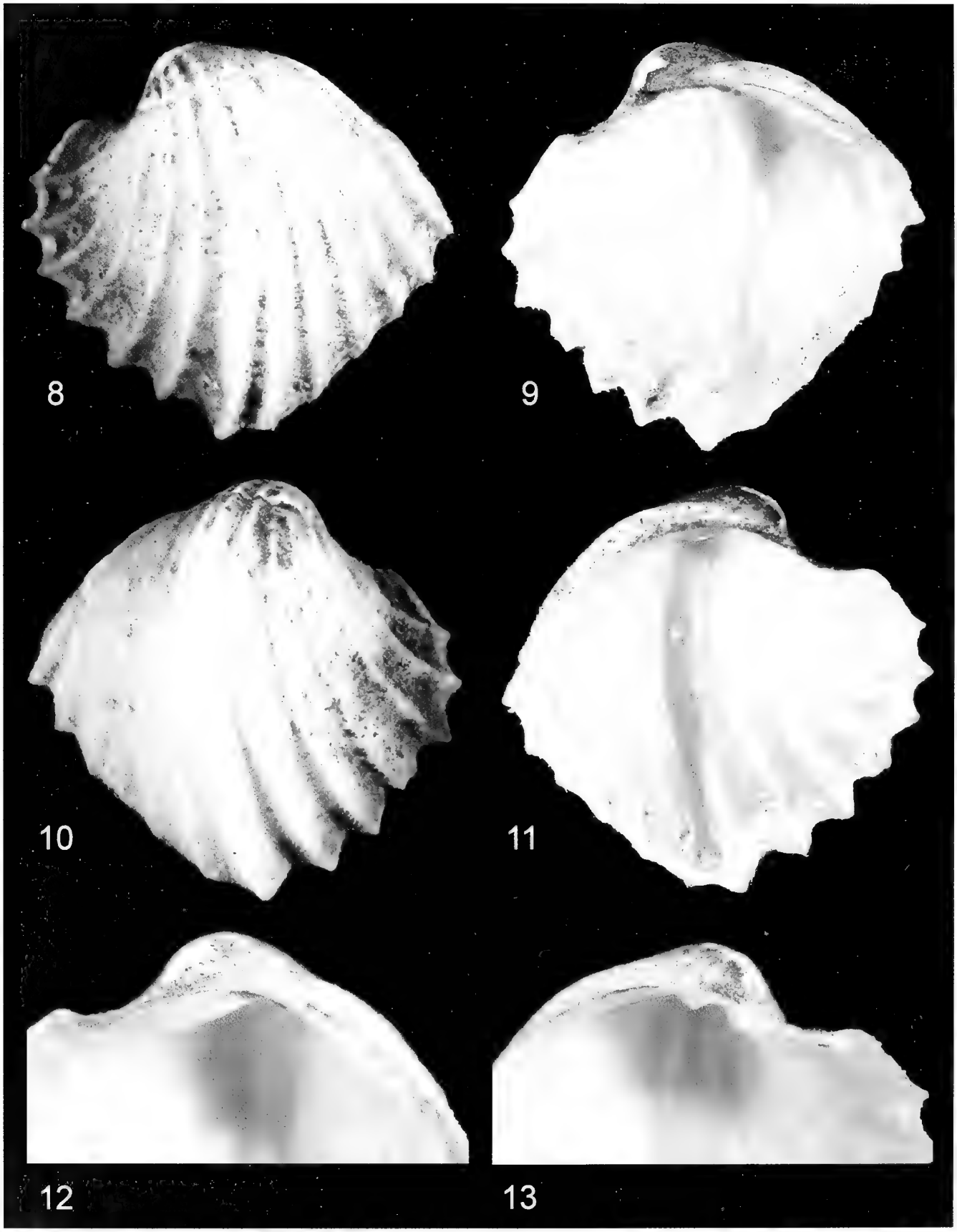

Figures 8–13. ***Spinosipella xui* new species**, holotype (TIO-BTS-MOL-1701). **8.** Exterior of left valve. **9.** Interior of left valve. **10.** Exterior of right valve. **11.** Interior of right valve. **12–13.** Details of hinges. **12.** Right valve. **13.** Left valve.

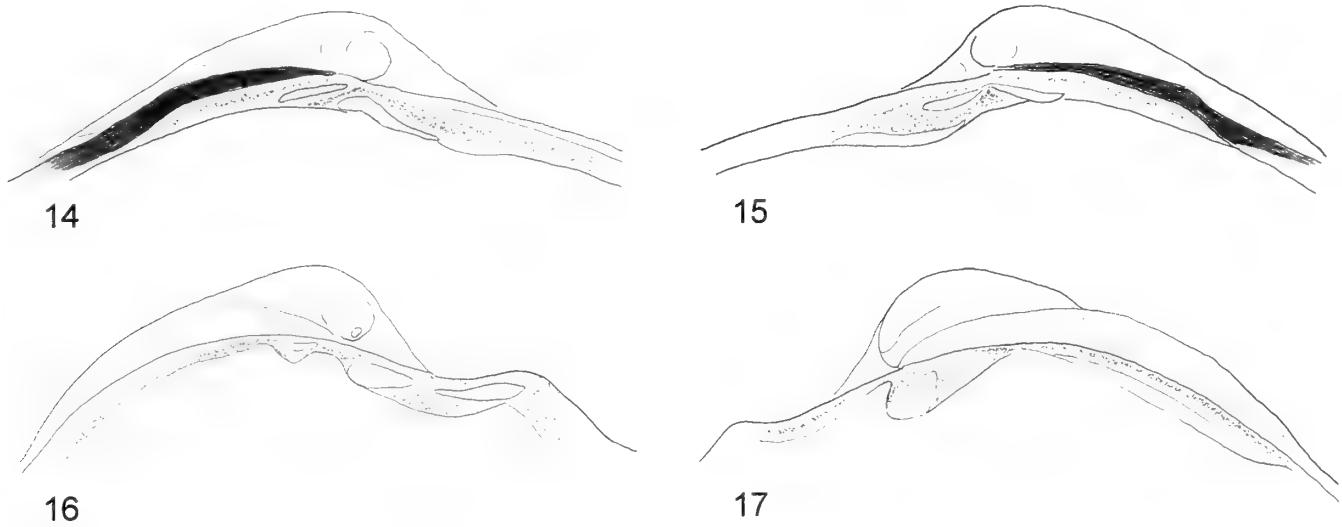

Figures 14–17. Semi-schematic line drawings of hinge plates. **14.** Left valve of ***Vesicomya rhombica* new species**. **15.** Right valve of ***Vesicomya rhombica* new species**. **16.** Left valve of ***Spinosipella xui* new species**. **17.** Right valve of ***Spinosipella xui* new species**.

overlapping left one, not gaping. Color chalky-white. Antero-dorsal margin short, depressed-concave; postero-dorsal margin sloping, slightly convex, about twice wider than anterior one; anterior and posterior ends forming abrupt right angles, with posterior one more protruded; ventral margin zigzag crenulated, rather convex, with antero-ventral margin almost vertical to postero-ventral, tips of zigzag coinciding with tips of each surface rib, tips corresponding to concavity of opposite valve; antero-dorsal margin almost parallel to postero-ventral, and postero-dorsal margin parallel to antero-ventral, forming lozenge-shaped shell outline. Umbones coiled, convex, projected, divergent, prosogyrate, situated in middle of dorsal margin. Outer surface with minute, opaque granulations forming irregular mosaics. Sculptured by strong, arched, widely spaced, 13 radial ribs triangular in cross-section, forming broad undulations on surfaces of valves and producing deeply plicate margins;

largest rib on middle forming prominent keel, dividing valve into anterior and posterior regions each with 6 ribs; ribs gradually becoming smaller from middle to shell ends. Lunule cordate, sunken, distinct, demarcated by incision. Escutcheon obscure, long, lanceolate. Internal surface of valves glossy, nacreous, white, iridescent, with undulations corresponding to ribs on external surface. Hinge plate narrow, under lunule. On right valve, hinge with large, stubby, tall, conical cardinal tooth, and long lamellar posterior lateral tooth parallel to postero-dorsal shell margin. On left valve, anterior cardinal tooth stout, long, extending along antero-dorsal margin, almost connected to smaller anterior lateral tooth under lunule; posterior cardinal tooth low, short and wedge-shaped; shallow socket between cardinal teeth, restricted to dorsal surface, and corresponding to the cardinal tooth of right valve. Anterior adductor muscle scars distinct, reniform, posterior adductor muscle scars elongate-ovate. Ligament opisthodetic, weak, almost imperceptible, nearly fused to periostracum along dorsal hinge margin; resilium brown, posterior to cardinal teeth. Pallial line very poorly defined.

Type Material: Holotype: TIO-BTS-MOL-1701 (Sta.QDN31) SL 4.7 mm, SH 4.3 mm, SW 3.8 mm.

Type Locality: Haima Methane Seep, muddy bottom, about 1,400 m depth off southern Hainan Island in the northern sector of the South China Sea.

Distribution: Known from the type locality.

Etymology: This species is dedicated to Prof. Fengshan Xu for his great contributions to Chinese malacology.

Remarks: The new species is allocated to the genus *Spinosipella* Iredale, 1930, due to its outline, a single strong cardinal tooth in the right valve, and a shallow socket in the left valve corresponding to the cardinal tooth of the right valve (Poutiers and Bernard, 1995). It is also noteworthy that the new species is different from other species of the genus in having a long thin lamellar posterior lateral tooth on the right valve. A long posterior lateral tooth on the right valve is also one of the characters typical of the genus *Trigonulina* d'Orbigny, 1853 (Poutiers and Bernard, 1995; Coan and Valentich-Scott, 2012). However, the lunule of the new species is sunken, distinct, and well-impressed, but not so deeply depressed as the two species of *Trigonulina*, i.e., the eastern Pacific *Trigonulina novemcostata* (A. Adams and Reeve, 1850) [= *Trigonulina pacifica* Jung, 1996= *Trigonulina hancocki* (Bernard, 1969)] and the western Atlantic *Trigonulina ornata* d'Orbigny, 1853. The lunules of these two species are deeply incised into the shell and overhung by umbones, and the hinge plates thickened. At the moment, only two species of *Spinosipella* with a tropical West

Pacific distribution are known (Simone and Cunha, 2008; Xu and Zhang, 2008). The number of radial ribs in the new species is much less than these two similar species, which have about 18–19 and 16–17 ribs, respectively. The new species has only 13 radial ribs, which is comparable to the Mediterranean *S. acuticostata* (Simone and Cunha, 2008). But *S. acuticostata* is higher than the new species, with stronger ribs and more prominent spines on the surface.

ACKNOWLEDGMENTS

The authors are grateful to Gene Coan, Steffen Kiel, and Elena Krylova for comments and suggestions on the manuscript, to Konstantin A. Lutaenko for providing some important literatures, to Xuebao He (Third Institute of Oceanography, Ministry of Natural Resources), who collected and loaned the material for this study, and to the scientific staff of the expedition and the ship crews of R/V HAI YANG SI HAO. This research was supported by the Basic Science Research Fund of Third Institute of Oceanography, MNR (No. TIO2016043), the National Special Project on Gas Hydrate of China (No. DD20190218), the Strategic Priority Research Program of the Chinese Academy of Sciences (No. XDA22050203), the Special Funds for Young Scholars of Taxonomy of the Chinese Academy of Sciences (No. ZSBR-009), and the Ocean Public Welfare Scientific Research Project, State Oceanic Administration of the People's Republic of China (No. 201505004-4).

LITERATURE CITED

Amano, K. and S. Kiel. 2007. Fossil vesicomyid bivalves from the North Pacific region. The Veliger 49: 270–293.

Arbizu, P.M. and S. Brix. 2008. Editorial: Bringing light into deep-sea biodiversity. Zootaxa 1866: 5–6.

Brökeland, W. and K.H. George. 2009. Editorial: Deep-sea taxonomy—a contribution to our knowledge of biodiversity. Zootaxa 2096: 6–8.

Chen, C., T. Okutani, Q. Liang, and J. Qiu. 2018. A noteworthy new species of the Family Vesicomyidae from the South China Sea (Bivalvia: Glossoidea). Venus 76: 29–37.

Coan, E.V. and P. Valentich-Scott. 2012. Bivalve seashells of tropical West America: Marine bivalve mollusks from Baja California to Peru, Part 1 & 2. Santa Barbara Museum of Natural History Monographs, 6. Santa Barbara Museum of Natural History, Santa Barbara, 1258 pp.

Cox, L.R. 1969. General features of Bivalvia. In: Moore, R. C. (ed.), Treatise on invertebrate paleontology Part N., Vol. 1, Mollusca 6, Bivalvia, Geological Society of America, Boulder, pp. 2–129.

Dall, W.H. 1886. Reports on the results of dredging, under the supervision of Alexander Agassiz, in the Gulf of Mexico (1877–78) and in the Carribean Sea (1879–80), by the U.S. Coast Survey steamer "Blake", Lieut.-Commander C.D. Sigsbee, U.S.N. and Commander J.R. Bartlett, U.S.N. commanding. XXIX. Report on the Mollusca. Part 1, Brachiopoda and Pelecypoda. Bulletin of the Museum of Comparative Zoölogy at Harvard College 12: 171–318.

Dall, W.H. and C.T. Simpson. 1901. The Mollusca of Porto Rico. Bulletin of the United States Fish Commission 20: 351–524.

Decker, C., K. Olu, R.L. Cunha, and S. Arnaud-Haond. 2012. Phylogeny and Diversification Patterns among Vesicomyid Bivalves. PLOS ONE 7: e33359.

Feng, D., J.-W. Qiu, Y. Hu, J. Peckmann, H. Guan, H. Tong, C. Chen, J. Chen, S. Gong, N. Li, and D. Chen. 2018. Cold seep systems in the South China Sea: An overview. Journal of Asian Earth Sciences 168: 3–16.

Filatova Z.A. 1971. On some mass species of bivalve molluscs from the ultra-abyssal zone of the Kurile-Kamtchatka Trench. Proceedings of the P. P. Shirshov Institute of Oceanology 92: 46–60.

Higo, S., P. Callomon, and Y. Gotō. 1999. Catalogue and bibliography of the marine shell bearing Mollusca of Japan: Gastropoda, Bivalvia, Polyplacophora, Scaphopoda. Elle Scientific Publications, Osaka, 749 pp.

Higo, S., P. Callomon, and Y. Gotō. 2001. Catalogue and bibliography of the marine shell bearing Mollusca of Japan: Gastropoda, Bivalvia, Polyplacophora, Scaphopoda. Type Figures. Elle Scientific Publications, 208 pp.

Huber, M. 2010. Compendium of Bivalves. A Full-Color Guide to 3300 of the World's Marine Bivalves: A Status on Bivalvia After 250 Years of Research. ConchBooks, Hackenheim, 901 pp.

Iredale, T. 1930. More notes on the marine Mollusca of New South Wales. Records of the Australian Museum 17: 384–407.

Johnson, S.B., E.M. Krylova, A. Audzijonyte, H. Sahling, and R.C. Vrijenhoek. 2017. Phylogeny and origins of chemosynthetic vesicomyid clams. Systematics and Biodiversity 15: 346–360.

Kamenev, G.M. 2019. Bivalve mollusks of the Kuril-Kamchatka Trench, Northwest Pacific Ocean: species composition, distribution and taxonomic remarks. Progress in Oceanography 176: 102127. doi: https://doi.org/10.1016/j.pocean.2019.102127

Knudsen, G.A. 1970. The Systematics and Biology of Abyssal and Hadal Bivalvia. Galathea Report 11: 1–241.

Krylova, E.M. and H. Sahling. 2010. Vesicomyidae (Bivalvia): Current taxonomy and distribution. PLoS ONE, 5: e9957.

Krylova, E.M. and R. Janssen R. 2006. Vesicomyidae from Edison Seamount (South West Pacific: Papua New Guinea: New Ireland fore-arc basin) (Bivalvia: Glossoidea). Archiv für Molluskenkunde 135: 231–261.

Krylova, E.M., G.M. Kamenev, I.P. Vladychenskaya, and N.B. Petrov. 2015. Vesicomyinae (Bivalvia: Vesicomyidae) of the Kuril–Kamchatka Trench and adjacent abyssal regions. Deep-Sea Research Part II, Topical Studies in Oceanography 111: 198–209.

Krylova, E.M., H. Sahling, and C. Borowski. 2018. Resolving the status of the families Vesicomyidae and Kelliellidae (Bivalvia: Venerida), with notes on their ecology. Journal of Molluscan Studies 84: 69–91.

Kuroda, T. 1952. On *Callocardia guttata* A. Adams and *Vesicomya katsuae*, n. sp. Venus 17: 1–5.

Liang, Q., Y. Hu, D. Feng, J. Peckmann, L. Chen, S. Yang, J. Liang, J. Tao, and D. Chen. 2017. Authigenic carbonates from newly discovered active cold seeps on the northwestern slope of the South China Sea: Constraints on fluid sources, formation environments, and seepage dynamics. Deep–Sea Research Part I: Oceanographic Research Papers 124: 31–41.

Liu, R. 2008. Checklist of Marine Biota of China Seas. Science Press, Beijing. 1267 pp.

Okutani, T. 2017. Marine Mollusks in Japan, Second Edition. Tokai University Press, Tokyo, 1375 pp.

Poutiers, J.M. and F. R. Bernard. 1995. Carnivorous bivalve molluscs (Anomalodesmata) from the tropical western Pacific Ocean, with a proposed classification and a catalogue of Recent species. Mémoires du Muséum national d'histoire naturelle (1993) 167: 107–187.

Simone, L.R.L. and C.M. Cunha. 2008. Revision of the genus *Spinosipella* (Bivalvia : Verticordiidae), with descriptions of two new species from Brazil. The Nautilus 122: 57–78.

Tsuchida, E. 1994. Bathyal mollusca collected by the R.V. Tansei-Maru from off Kochi Prefecture (1) Bivalvia. Bulletin of Marine Sciences & Fisheries, Kochi University 14: 73–89.

Valdés, F., J. Sellanes, and G. D'Elía. 2012. Phylogenetic position of vesicomyid clams from a methane seep off central Chile (~ 36 S) with a molecular timescale for the diversification of the Vesicomyidae. Zoological Studies 51: 1154–1164.

von Cosel, R. and C. Salas. 2001. Vesicomyidae (Mollusca: Bivalvia) of the genera *Vesicomya*, *Waisiuconcha*, *Isorropodon* and *Callogonia* in the eastern Atlantic and the Mediterranean. Sarsia 86: 333–366.

Woodring, W.P. 1925. Miocene Mollusca from Bowden Jamaica, pelecypods and scaphopods. Carnegie Institution of Washington Publication 366: 1–564.

Xu, F. and S. Shen. 1991. A new species of Vesicomyidae from Nansha Islands waters. In: Papers on Marine Biology of Nansha Islands and Adjacent Seas. Beijing: China Ocean Press, 1, pp.164–166.

Xu, F. and S. Zhang. 2008. An Illustrated Bivalvia Mollusca Fauna of China Seas. Science Press, Beijing, 336 pp.

Sponsored in part by the State of Florida, Department of State, Division of Cultural Affairs and the Florida Council on Arts and Culture

THE NAUTILUS

Volume 133
2019

AUTHOR INDEX

NEW TAXA PROPOSED IN VOLUME 133

GASTROPODA

BIVALVIA

REVIEWERS FOR VOLUME 133

Becker, Lothar
Beu, Alan G.
Bieler, Rüdiger
Breure, Abraham S.H.
Carew, James
Coan, Eugene V.
Cowie, Robert H.
Cummings, Kevin
Egorov, Roman
Fedosov, Alexander
Giribet, Gonzalo
Harasewych, M.G.
Hayes, Kenneth A.
Herbert, Gregory
Hryniewicz, Krzysztof
Jenkins, Robert G.
Kabat, Alan
Kantor, Yuri
Kiel, Steffen
Kohler, Frank
Krylova, Elena M.
Lee, Harry G.
Little, Crispin
Mikkelsen, Paula M.
Nielsen, Sven
Nützel, Alexander
Páll-Gergely, Barna
Pearce, Timothy A.
Pfeiffer, John
Portell, Roger W.
Rolán, Emilio
Slapcinsky, John
Vermeij, Geerat J.
Vilvens, Claude

INSTRUCTIONS TO AUTHORS

The Nautilus publishes articles on all aspects of the biology, paleontology, and systematics of mollusks. Manuscripts describing original, unpublished research and review articles will be considered. Brief articles, not exceeding 1000 words, will be published as Research Notes and do not require an abstract.

Manuscripts: Each original manuscript and accompanying illustrations should be submitted to the editor via e-mail. Authors should follow the general recommendations of Scientific Style and Format—The CSE Manual for Authors, Editors, and Publishers, available from the Council of Science Editors at http://www.scientificstyleandformat.org/Home.html.

The first mention of a scientific name in the text should be accompanied by the taxonomic authority, including year. Metric, not English, units are to be used. The sequence of sections should be Title, Author(s) and Affiliations, Abstract, Additional Keywords, Introduction, Materials and Methods, Results, Discussion, Conclusions, Acknowledgments, Literature Cited, Tables, Figure Captions, Figures. If the author for correspondence is not the senior author, please indicate in a footnote. The abstract should summarize in 250 words or less the scope, main results, and conclusions of the article. Abstracts should be followed by a list of additional keywords. All references cited in the text must appear in the Literature Cited section and vice-versa. Please follow a recent issue of *The Nautilus* for bibliographic style, noting that journal titles must be unabbreviated. Information on plates and figures should be cited only if not included within the pagination of cited work. Tables must be numbered and each placed on a separate page. If in doubt, please follow a recent issue of the journal for sequence of sections and other style requirements.

Illustrations: Illustrations are rendered either at full-page width (maximum width 17 cm) or column width (maximum width 8.2 cm). Please take these dimensions into consideration when preparing illustrations. Page-width illustrations ideally should span the entire width of printed page (17 cm). "Tall" page-width illustrations should be avoided, square or "landscape" formats work better. Please design plates accordingly, such that there will be enough space left at the bottom of printed page for plate caption. (Digital technology has made this task much easier.)

All line drawings must be in black, clearly detailed, and completely labeled. Abbreviation definitions must be included in the caption. Line drawings must be high resolution fi les at least 600 dpi (dots per inch) resolution at actual size. Standard digital formats for line drawings include .tif, .bmp, .psd, .eps, and .pdf.

Photographs may be submitted in black-and-white or color, preferably in RGB mode if in color. Standard digital formats for photographs include .tif, .psd, .jpg, or .pdf. Photographs must be high resolution files at least 300 dpi resolution at actual (printed) size.

If more than one figure is included in an illustration, all figures are to be consecutively numbered (Figures 1, 2, 3, . . . , NOT Figures 1A, 1B, 1C, . . . , NOR Plate 1, Figure 1, . . .). In illustrations with more than one figure, make sure that blank areas between figures should be kept to a minimum, thereby allowing for more area for each individual figure.

Compressed (e.g., .jpg) or other low-resolution file formats may be used to facilitate original submission and the review process, but may not be acceptable at final submission (see below).

Types and Voucher Specimens: Deposition of the holotype in a recognized institutional, public collection is a requirement for publication of articles in which new species-level taxa are described. Deposition of paratypes in institutional collections is strongly recommended, as is the deposition of representative voucher specimens for all other types of research work.

The Editorial Process: Upon receipt, all manuscripts are assigned a number and acknowledged. The editor reserves the right to return manuscripts that are substandard or not appropriate in scope for journal. Manuscripts deemed appropriate for the journal will be sent for critical review to at least two reviewers. The reviewers' recommendations will serve as basis for rejection or continuation of the editorial process. Reviewed manuscripts will be sent back to authors for consideration of the reviewers comments. The revised version of the manuscript may at this point be considered accepted for publication by the journal.

Final Submission: Authors of accepted manuscripts are required to submit a final version to the editor at jleal@shellmuseum.org. High-resolution image files may be sent to the editor at this stage.

Proofs: After typesetting, proofs will be sent to the author. Author should read proofs carefully and send corrections to the editor within 48 hours. Changes other than typesetting errors will be charged to the author at cost.

Offprints: An order form for offprints will accompany the proofs. Offprints will be ordered directly from the editor. Authors with institutional, grant, or other research support will be asked to pay for page charges at the rate of $60 per page.

More information at http://shellmuseum.org/learn/the-nautilus.